

---

# MILO: MODEL-AGNOSTIC SUBSET SELECTION FRAMEWORK FOR EFFICIENT MODEL TRAINING AND TUNING

---

Krishnateja Killamsetty<sup>1,2,\*</sup>, Alexandre V. Evfimievski<sup>2</sup>, Tejaswini Pedapati<sup>2</sup>  
Kiran Kate<sup>2</sup>, Lucian Popa<sup>2</sup>, Rishabh Iyer<sup>1</sup>

<sup>1</sup> The University of Texas at Dallas

<sup>2</sup> IBM Research

{krishnateja.killamsetty, rishabh.iyer}@utdallas.edu  
{evfimi, tejaswinip, kakate, lpopa}@us.ibm.com

February 1, 2023

## ABSTRACT

Training deep networks and tuning hyperparameters on large datasets is computationally intensive. One of the primary research directions for efficient training is to reduce training costs by selecting well-generalizable subsets of training data. Compared to simple adaptive random subset selection baselines, existing intelligent subset selection approaches are not competitive due to the time-consuming subset selection step, which involves computing model-dependent gradients and feature embeddings and applies greedy maximization of submodular objectives. Our key insight is that removing the reliance on downstream model parameters enables subset selection as a pre-processing step and enables one to train multiple models at no additional cost. In this work, we propose MILO, a model-agnostic subset selection framework that decouples the subset selection from model training while enabling superior model convergence and performance by using an easy-to-hard curriculum. Our empirical results indicate that MILO can train models  $3 \times -10 \times$  faster and tune hyperparameters  $20 \times -75 \times$  faster than full-dataset training or tuning without compromising performance.

## 1 Introduction

In recent years, deep learning has achieved tremendous success in many machine learning tasks, including natural language processing, computer vision, and speech recognition. Deep learning’s success is partly attributed to the availability of massive training datasets and the ability to train vast neural networks. However, training deep models on massive datasets is computationally demanding, incurs significant financial expenses, and generates considerable CO2 emissions [62, 58]. Bartoldson et al. [2] have provided an excellent summary of various research directions previously explored, such as data subset selection, curriculum learning, model architecture enhancements, and optimization algorithm enhancements, to improve model convergence and reduce training time and costs. In this work, we focus on selecting useful, generalizable data subsets for the efficient training of deep neural networks. Recent studies [64, 5, 21] have shown that existing training datasets are often redundant. This suggests that training on a redundancy-free, informative subset can achieve performance similar to full data training.

To identify informative data samples, recent works have employed metrics such as prediction uncertainty [8], prediction flips [64, 68], loss [42], or gradient/gradient-norm [20, 47, 28, 27, 29] computed by using the downstream machine learning model or its lightweight surrogate [8]. To compute these measures reliably, a converged model is necessary ahead of time, which negates the aim of efficient training. Existing subset selection algorithms [47, 28, 27, 29, 30, 54] for efficient training address this issue by regularly updating the subset as the model-dependent metrics for each sample change.

**Drawbacks of Model-Dependent Subset Selection:** Despite their theoretical guarantees, existing subset selection approaches are computationally inefficient compared to adaptive random subset selection (selection of random subsets

---

\* A portion of this work was completed while Krishnateja was an intern at IBM Research.

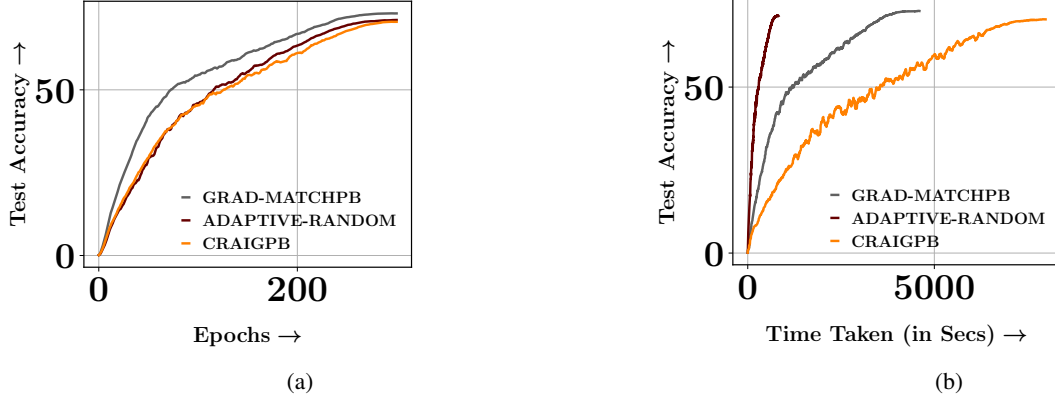


Figure 1: Sub-figure (a) and Sub-figure (b) show convergence of the ResNet18 model trained using 10% subsets selected using Adaptive-Random, CRAIGPB, and GRADMATCHPB on CIFAR100 dataset w.r.t epochs and time respectively. Here, we select a new subset every epoch for all the considered strategies.

at regular intervals). This is because they are downstream model dependent and often require the computation of sample metrics such as gradients prior to each subset selection step. For example, Figure 1 illustrates the convergence of the ResNet18 model on the CIFAR100 datasets in terms of time and epochs, using 10% subsets selected every epoch by GRADMATCHPB [27], a SOTA data subset selection strategy for efficient training, CRAIGPB [47], and Adaptive-Random (where a new 10% subset is randomly selected at regular intervals). We select a new subset every epoch to showcase the maximal performance that can be achieved by GRADMATCHPB and CRAIGPB. Results show that GRADMATCHPB provides faster epoch convergence than Adaptive-Random and CRAIGPB when selecting a new subset every epoch. However, due to the need to perform a computationally expensive subset selection step every epoch, both GRADMATCHPB and CRAIGPB are highly inefficient in terms of training time. In their studies, Killamsetty et al. [27] and Mirzasoleiman et al. [47] recommended selecting a new subset every  $R$  epochs to improve training efficiency, but at the expense of the model’s convergence rate. Finally, model-dependent subset selection necessitates the compute-expensive subset selection step each time a new model is trained.

**Model-Agnostic Subset Selection:** Our central insight is that a model-agnostic subset selection framework can avoid computationally expensive subset selection steps during model training, relegating subset selection to the preprocessing phase. By pre-selecting subsets and saving them as metadata in each dataset, we may train numerous models without additional costs, amortizing the subset selection costs. In this work, we attempt to answer the following question: *Can we develop a model-agnostic subset selection approach that selects new subsets in a negligible amount of time yet achieves superior model convergence while sacrificing little test accuracy or generalization performance?*

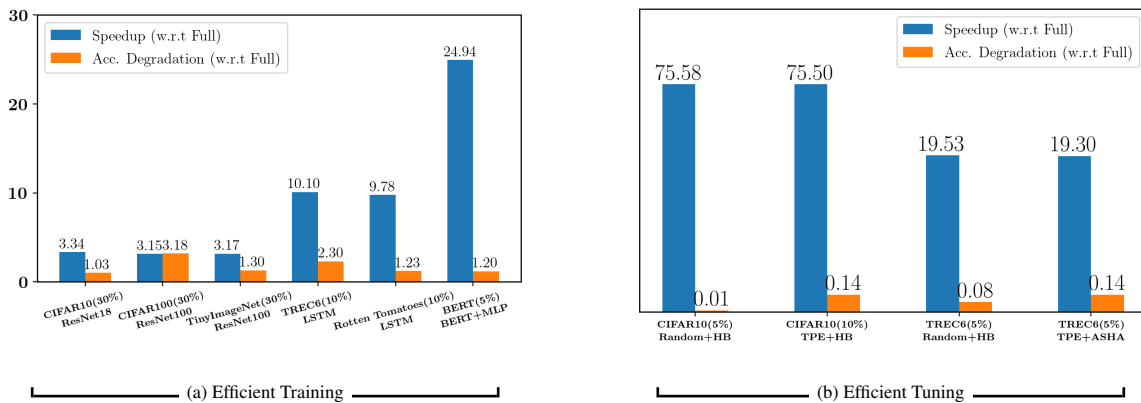


Figure 2: Comparison of MILO with full data training and tuning: We contrast the accuracy degradation with speedup compared to the full data training or full data tuning. We observe speedups of around  $3 \times -10 \times$  speedup with around 1.5% accuracy drop. For hyper-parameter tuning, we observe  $20 \times -75 \times$  speedup compared to full data tuning with less than 0.15% accuracy drop.

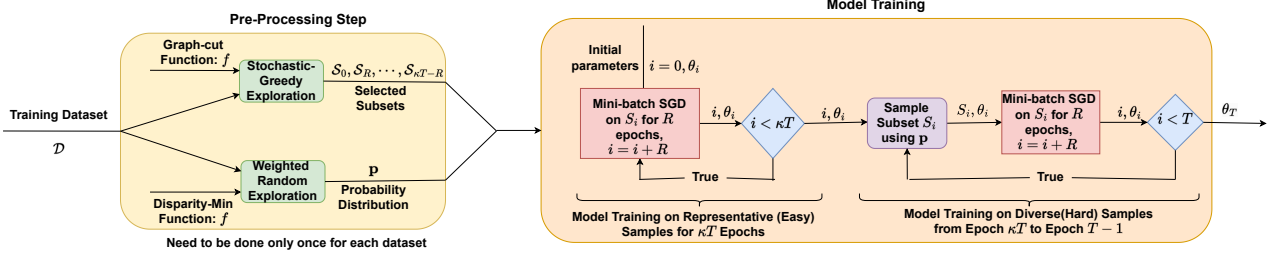


Figure 3: Block Diagram of MILO for model training using a curriculum of easy-to-hard data subsets, where data subsets are changed every  $R$  epochs of (stochastic) gradient descent, and the gradient descent updates are performed on the selected subsets.

## 1.1 Contributions

The contributions of our work can be summarized as follows:

### 1.1.1 MILO Framework

In this work, we propose MILO, a model-agnostic subset selection framework for efficient model training and tuning. MILO utilizes submodular measures [14, 23] which capture higher-order interactions between data samples for subset selection. We utilize pre-trained large language models [55] and pre-trained vision transformers [25] as feature encoders and compute the sample metrics. This computation is not dependent on the downstream model making MILO model-agnostic. Figure 3 presents the pictorial depiction of MILO for model training, which consists of two steps: a) a pre-processing step that includes the selection of multiple subsets from the training dataset through "Stochastic-Greedy Exploration (SGE)" (c.f., Section 3.4.1) and construction of probability distribution over the entire dataset for subset sampling through "Weighted Random Exploration (WRE)" (c.f., Section 3.4.2); b) a model training scheme that involves training the model on a curriculum of easy-to-hard subsets (c.f., Section 3.4.3) using the subsets selected and the probability distribution constructed in the pre-processing step. We also present a class-wise partitioning trick to minimize the memory footprint of MILO significantly. (c.f., Section 3.5)

### 1.1.2 Effectiveness of MILO

We empirically demonstrate the effectiveness of MILO framework for efficient training and hyper-parameter tuning through extensive experiments on multiple real-world datasets. We summarize the speedup vs. relative performance achieved by MILO compared to full data training in Figure 2. More specifically, we demonstrate that MILO can train models  $3\times-10\times$  faster and tune hyper-parameters  $20\times-75\times$  faster than full dataset training or tuning with minimal performance loss. MILO also consistently outperforms the considered subset selection baselines.

## 1.2 Related Work

In recent years, data-subset selection approaches have found success in various applications of machine learning like speech recognition [66, 65, 41], machine translation [32], active learning [59, 1, 33], hyper-parameter tuning [30], semi-supervised learning [29], continual learning [63], domain adaptation [19], and computer vision [22]. A recent empirical study [5] showed that datasets often contain semantic redundancies that can be removed during training without affecting performance. To that extent, data pruning approaches [64, 51, 61] developed principled selection criteria for pruning redundant samples prior to model training with minimal loss in performance. However, both the existing data pruning and compute-efficient learning approaches are model-dependent, making them computationally expensive. In contrast, our method is model agnostic and capable of finding high-quality subsets by utilizing the capabilities of large pre-trained transformer models and can achieve superior model convergence by utilizing an easy-to-hard curriculum starting from representative to diverse subsets during training.

## 2 Preliminaries

### 2.1 Notation

We briefly describe the notation for various variables that will be used throughout the remainder of this section. Denote the training dataset as  $\mathcal{D} = \{(x_j, y_j)\}_{j=1}^m$  with  $m$  data points. Let  $S$  be the subset of the training dataset on which the

downstream model is trained. Let the feature encoder be denoted as  $g : X \rightarrow Z$  that transforms the input from the feature space  $X$  to an embedding space  $Z$ . Let the downstream model parameters be characterized by  $\theta$ . We subscript the changing variables like model parameters  $\theta$  and subset  $\mathcal{S}$  with the timestep  $t$  to denote their specific values at that timestep. Let the subset size be denoted as  $k$ .

## 2.2 Submodular Functions

Let  $\mathcal{U}$  be a dataset of  $n$  points  $\mathcal{U} = \{1, 2, 3, \dots, n\}$  and  $f : 2^{\mathcal{U}} \rightarrow \mathbb{R}$  be a set function mapping sets to real values, i.e., for a set  $\mathcal{A} \subseteq \mathcal{U}$ ,  $f(\mathcal{A})$  provides a real-valued score for  $\mathcal{A}$ . Formally, a function  $f$  is submodular [14] if for  $x \in \mathcal{U}$ ,  $f(\mathcal{A} \cup x) - f(\mathcal{A}) \geq f(\mathcal{B} \cup x) - f(\mathcal{B})$ ,  $\forall \mathcal{A} \subseteq \mathcal{B} \subseteq \mathcal{U}$  and  $x \notin \mathcal{B}$ . Moreover, submodular gain  $f(x|\mathcal{U})$  is defined as the difference between the submodular set function value of set  $\mathcal{U} \cup x$  and the set function value of set  $\mathcal{U}$ , i.e.,  $f(x|\mathcal{U}) = f(\mathcal{U} \cup x) - f(\mathcal{U})$ . Finally, a function  $f$  is said to be monotone if  $f(\mathcal{A}) \leq f(\mathcal{B})$  whenever  $\mathcal{A} \subseteq \mathcal{B}$ . While most general discrete maximization problems are NP-hard, they can be approximately solved if the set function  $f$  being maximized is submodular. Monotone Submodular functions admit a constant factor approximation of  $1 - \frac{1}{e}$  [48] when maximized under a cardinality constraint using a simple greedy algorithm.

## 2.3 Subset Selection Formulation

The standard subset selection problem can be formulated as the maximization of a set function  $f$  subject to a budget constraint  $k$ :

$$\mathcal{S}^* = \arg \max_{\mathcal{S}: \mathcal{S} \subseteq \mathcal{D}, |\mathcal{S}|=k} f(\mathcal{S}) \quad (1)$$

If the set function  $f$  is monotone submodular, then the above optimization problem can be solved with approximation guarantees.

# 3 Development of MILO

In this section, we explain the theoretical and empirical considerations that led to the development of MILO. Our primary goal for the new subset selection approach is that it selects a new subset in a negligible amount of time and provides superior model convergence and performance within a stated period.

## 3.1 Choice of Feature Encoders

As described in Equation (1), the standard subset selection problem involves the maximization of the set function  $f$  under a budget constraint. Most set functions  $f$  require the computation of a similarity kernel  $\mathcal{K}$  [23] to capture higher-order interactions between data samples. We need informative encodings of samples for such computation. Our first design choice was to utilize existing pre-trained language models or vision transformers as feature encoders  $g$  because they provide a greater level of contextualization, are more expressive and generalizable, and can be extrapolated [55, 25]. It also eliminates the need for downstream machine-learning models to compute sample representations. We analyze the effectiveness of different language models or vision transformers as feature encoders for subset selection in Appendix 4.6.1.

## 3.2 Optimal Subset Composition

The immediate question is which set function should be used to perform subset selection. More specifically, *what qualities are essential for the subset in order for the model to perform well?* To determine the essential characteristics that should be present in the selected subsets for effective model training, we compare the empirical performance of different set functions that model the following subset qualities:

- *Representation*: measures how well the subset represents the entire dataset, for example, ensuring that the subset contains more samples from dense regions than sparse regions. Such subsets tend to have "easier" data samples. For modeling representation, we considered facility location and graph-cut set functions.
- *Diversity*: measures how different the data samples in the subset are from each other, for example, ensuring that the subset contains very different samples. Such subsets tend to have "harder" data samples. For modeling diversity, we consider the disparity-sum and disparity-min set functions.

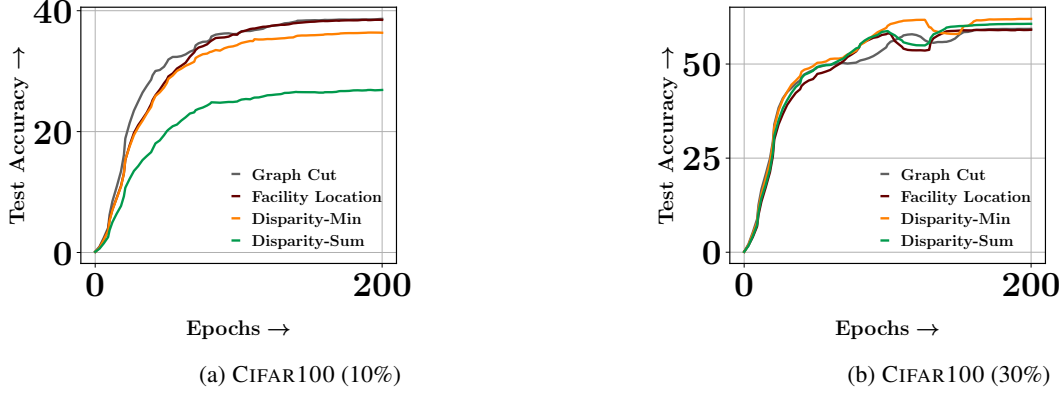


Figure 4: Performance of ResNet18 model trained on 10% and 30% subsets of the CIFAR100 dataset selected by maximizing different set functions.

Apart from disparity-min, all other set functions considered are submodular. Even though disparity-min is not submodular, it has been empirically demonstrated to operate well with the conventional greedy approach [9] and was therefore examined. We provide instantiations of the considered set functions in Appendix C. Figure 4 demonstrates the performance of a ResNet18 model trained on 10% and 30% subsets of the CIFAR100 dataset, respectively, by maximizing different set functions. Results show that when using large subset sizes like 30% or greater, subsets selected with diversity functions disparity-min and disparity-sum result in higher model performance, whereas for small subset sizes of 10% or less, subsets selected with representation functions graph cut and facility location result in higher model performance. This observation also agrees with the recent findings of Sorscher et al. [61].

### 3.3 Issue with using fixed data subsets

A significant disadvantage of training models using *fixed* data subsets is the requirement of large data subsets (about 70% or more) to achieve similar accuracy to full data training, resulting in longer training times. However, suppose the objective is to achieve the best performance within a specified timeframe. In that case, the model must also explore data instead of simply relying on a fixed subset of data. For instance, the ResNet101 model trained on a fixed 10% random subset of the CIFAR10 dataset for 200 epochs yielded 66.9% test accuracy. In contrast, the ResNet101 model achieved 87.54% test accuracy when trained on an adaptive 10% subset of CIFAR10 data for 200 epochs, where a new subset is randomly selected after each epoch. Although random data exploration is simple but an empirically successful method of exploring data, it is not the most effective method because the selected random subsets are prone to redundancy. It is therefore essential to develop a strategy that achieves a balance between *Subset Exploration and Subset Exploitation*.

### 3.4 Informative Data Exploration

To achieve a balance between exploration and exploitation, we must train our models on subsets that are small, highly informative, yet randomly sampled. A performant subset selection approach would combine training samples from all parts of the dataset without undue bias. An ideal formulation for informative data subset exploration is as follows:

$$P(\mathcal{S}) \propto \exp(\beta \cdot f(\mathcal{S})) \text{ subject to } |\mathcal{S}| = k \quad (2)$$

where  $P(\mathcal{S})$  denotes the probability of sampling the subset  $\mathcal{S}$ , function  $f$  is our set quality measure, and  $\beta > 0$  is inverse temperature [15]. If Equation (2) holds, we explore higher quality subsets more frequently but otherwise show no preference in the points we sample. Ideally, we want to select a new subset for every epoch by sampling it from this probability distribution. Constructing a naïve sampler according to Equation (2) requires a combinatorial number of set function evaluations. For sampling  $P(\mathcal{S})$  without the size constraint, Gotovos et al. [15] proposed a Gibbs sampling approach for marginal inference with a polynomial mixing time in  $|\mathcal{D}|$ . However, to enforce  $|\mathcal{S}| = k$ , the proposed Gibbs sampler needs to be modified, which includes swapping one data point for another at each step. For a uniformly random data point, when the current subset has close to optimal  $f(\mathcal{S})$  value, the swapping probability would usually be close to 0 because the swapping worsens  $f(\mathcal{S})$ , making the modified Gibbs sampler reject the majority of proposed swaps and leading to considerable mixing times. We leave this extension of Gotovos et al. [15] to future work. Below, we present two scalable alternatives to data exploration with varying exploration-to-exploitation ratios.

**Algorithm 1** SGE**Require:** Train set:  $\mathcal{D}$ ; Subset Size:  $k$ ; Set function:  $f$ ;  $\epsilon = 1e - 2$ ; Number of Subsets:  $n$ \*\*\* Sampling  $n$  subsets using stochastic-greedy \*\*\*

---

```

1: for  $i \in 0, \dots, n - 1$  do
2:    $\mathcal{S}_i = \emptyset$  // Initialize empty subset
3:    $s = \frac{|\mathcal{D}|}{k} \log(\frac{1}{\epsilon})$  // Random subset size for stochastic-greedy algorithm
4:   for  $j \in 0, \dots, k - 1$  do
5:      $R \leftarrow$  A random subset obtained by sampling  $s$  elements from  $\mathcal{D} \setminus \mathcal{S}_i$ 
6:      $e = \arg \max_{e \in R} f(A \cup e) - f(A)$ 
7:      $\mathcal{S}_i = \mathcal{S}_i \cup \{e\}$ 
8:   end for
9:   Return selected subsets  $\mathcal{S}_0, \dots, \mathcal{S}_{n-1}$ 
10: end for

```

---

**3.4.1 Stochastic-Greedy Exploration (SGE)**

The first method we employ to explore the data is identifying multiple subsets with high function values. Then, we train the downstream model based on those selected subsets by changing the subsets every  $R$  epochs. Due to its focus on subsets with high function values, this approach emphasizes exploitation rather than exploration. To select  $n$  subsets  $\mathcal{S}_1, \mathcal{S}_2, \dots, \mathcal{S}_n$  from dataset  $\mathcal{D}$  with high set function values, we employ the stochastic greedy algorithm [46] for maximization of the set function  $f$  and repeat the maximization  $n$  times.

$$\mathcal{S}_1, \mathcal{S}_2, \dots, \mathcal{S}_n \leftarrow \text{SGE}(f, \mathcal{D}, k) \quad (3)$$

The randomness of the stochastic greedy algorithm allows us to choose a different subset with an approximate guarantee of  $\mathcal{O}(1 - \frac{1}{e} - \epsilon)$  every time. We present a detailed pseudocode of the "SGE" in Algorithm 1. In our experiments, we use an  $\epsilon$  of value 0.01 for stochastic greedy maximization.

**Algorithm 2** GreedySampleImportance Algorithm**Require:** Train set:  $\mathcal{D}$ ; Subset Size:  $k$ ; Set function:  $f$ ;

---

```

1:  $\mathcal{S} = \emptyset$  // Initialize empty subset
2: Initialize gains vector of dimension  $|\mathcal{D}|$  to zeros  $\mathbf{g} = \vec{0}$  *** Calculate greedy informative gains for each element ***
3: for  $j \in 0, \dots, |\mathcal{D}| - 1$  do
4:    $g = \max_{e \in \mathcal{D} \setminus \mathcal{S}} f(A \cup e) - f(A)$ 
5:    $e = \arg \max_{e \in \mathcal{D} \setminus \mathcal{S}} f(A \cup e) - f(A)$ 
6:    $\mathbf{g}[e] = g$ 
7: end for
8: Return gains vector  $\mathbf{g}$ 

```

---

**3.4.2 Weighted Random Exploration (WRE)**

In this approach, we explore the data by constructing a multinomial probability distribution  $\mathbf{p}$  over the entire dataset  $\mathcal{D}$  and sampling a subset  $\mathcal{S}$  of size  $k$  every  $R$  epochs from the constructed probability distribution without replacement. Our main idea is to use a weighted random sampling approach [13] by assigning each data sample the normalized set function gains associated with it during greedy maximization as its weight. More specifically, we maximize the set function  $f$  over the entire dataset  $\mathcal{D}$  greedily and store the set function gains associated with each data sample  $e$  at the moment of its greedy inclusion as its importance score  $g_e$ . Accordingly, if  $\mathcal{S}$  represents the subset selected greedily so far, and  $e$  represents the next greedy optimal data sample to be added, the set function gain value of  $e$  is  $f(\mathcal{S} \cup e) - f(\mathcal{S})$ .

$$\mathbf{g} = [g_1, g_2, \dots, g_m] \leftarrow \text{GreedySampleImportance}(f, \mathcal{D}) \quad (4)$$

As shown in Equation (5), we normalize the importance scores  $\mathbf{g}$  and construct the probability distribution  $\mathbf{p}$  over the training set  $\mathcal{D}$  by employing the second order Taylor-Softmax function [10] over the importance scores.

$$\mathbf{p} = \text{Taylor-Softmax}(\mathbf{g}) = \left[ \frac{1 + g_i + 0.5g_i^2}{\sum_{j=1}^m 1 + g_j + 0.5g_j^2} \right]_{i=1}^m \quad (5)$$

Due to the diminishing gains property of submodular functions, when  $f$  is submodular, the set function gain of elements added in early iterations is greater than that of elements selected in later iterations. In addition, the generated probability distribution  $\mathbf{p}$  guarantees that informative samples are assigned a higher probability than less informative ones. Depending on the set function used, information can be representativeness or diversity of the subset. Importantly, sampling from the probability distribution  $\mathbf{p}$  allows for exploring less informative samples while selecting informative samples more frequently. Once the probability distribution  $\mathbf{p}$  is constructed, sampling new subsets from the constructed multinomial probability distribution is as fast as random subset selection. We use the probability distribution  $\mathbf{p}$  to sample new subsets of size  $k$  every  $R$  epochs by sampling  $k$  points (without replacement). We present a detailed pseudocode of the greedy sample importance estimation in Algorithm 2.

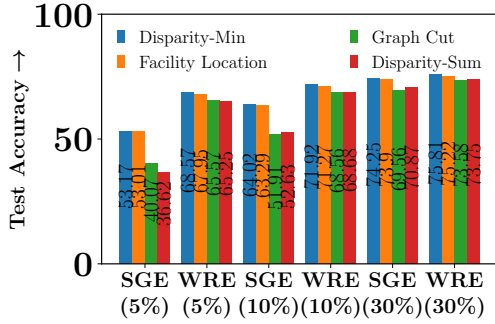


Figure 5: Figure shows the performance of the ResNet18 model trained on 5%, 10%, and 30% subsets of the CIFAR100 dataset using SGE and WRE approaches with different set functions.

**SGE vs. WRE:** Figure 5 demonstrates that training the ResNet18 model with WRE(that emphasizes more exploration) results in better performance than using SGE(that emphasizes more exploitation) and fixed data subsets(pure exploitation). Further, using Disparity-Min as a set function performs better than other set functions for both exploration approaches. Even though WRE performs better than SGE, we made a critical empirical observation highlighting that SGE with Graph-cut results in superior model convergence in initial iterations. Figures 6,7 illustrate the superior model convergence of SGE using graph-cut (easy samples) in initial training iterations compared to the WRE using disparity-min (hard samples), WRE using graph-cut (easy samples) and SGE using facility location (easy samples) across multiple datasets and subset sizes. We give a detailed explanation of why SGE with graph-cut results in superior initial convergence than SGE with facility location and WRE with graph-cut even though all of these approaches try to select easy/representative samples below.

**SGE (Graph-Cut) vs SGE (Facility Location)** Figure 6 shows the model convergence curves trained using SGE with Graph-Cut and SGE with Facility Location on various datasets using different subset sizes. Results show that SGE with Graph-Cut achieves faster initial convergence than SGE with Facility Location across all the datasets considered and for different subset sizes. The reason why SGE with Graph-Cut gives superior initial model convergence compared to SGE with Facility Location is that the sum-sum formulation in graph-cut( Equation (9)), as opposed to the sum-max formulation in facility location( Equation (8)), results in the selection of more number of easy samples. More specifically, with the sum-max formulation for facility location, having a single representative sample of data from each cluster in the dataset is sufficient to achieve a high facility location value for that cluster and having a representative sample from all the clusters in the dataset leads to further maximization of facility location values. This prevents the selection of samples only from densely populated regions while achieving broader coverage of the selected dataset in the facility location. Whereas, with the sum-sum formulation of the graph-cut function, selecting more samples from dense regions, leads to the high graph-cut function values. Thus, graph-cut can result in the selection of subsets consisting of higher number of easy samples from very dense regions in the dataset than facility location.

**SGE (Graph-Cut) vs. WRE (Graph-Cut)** Figure 7 shows the model convergence curves trained using SGE with Graph-Cut and WRE with Graph-Cut on various datasets using different subset sizes. Results show that SGE with Graph-Cut achieves faster initial convergence than WRE with Graph-Cut across all the datasets considered and for different subset sizes. The reason why SGE with Graph-Cut gives superior initial model convergence compared to WRE with Graph-Cut is that SGE emphasizes more exploitation than WRE. More specifically, SGE results in selecting subsets with high set function values because of the approximation guarantees of the stochastic-greedy algorithm [46]. Whereas with WRE, there is no guarantee that the sampled subsets using the constructed probability distribution  $\mathbf{p}$  have set function values. Since subsets with higher Graph-Cut function values correspond to subsets with more easy samples, SGE with Graph-Cut achieves superior model convergence than SGE with Facility Location.

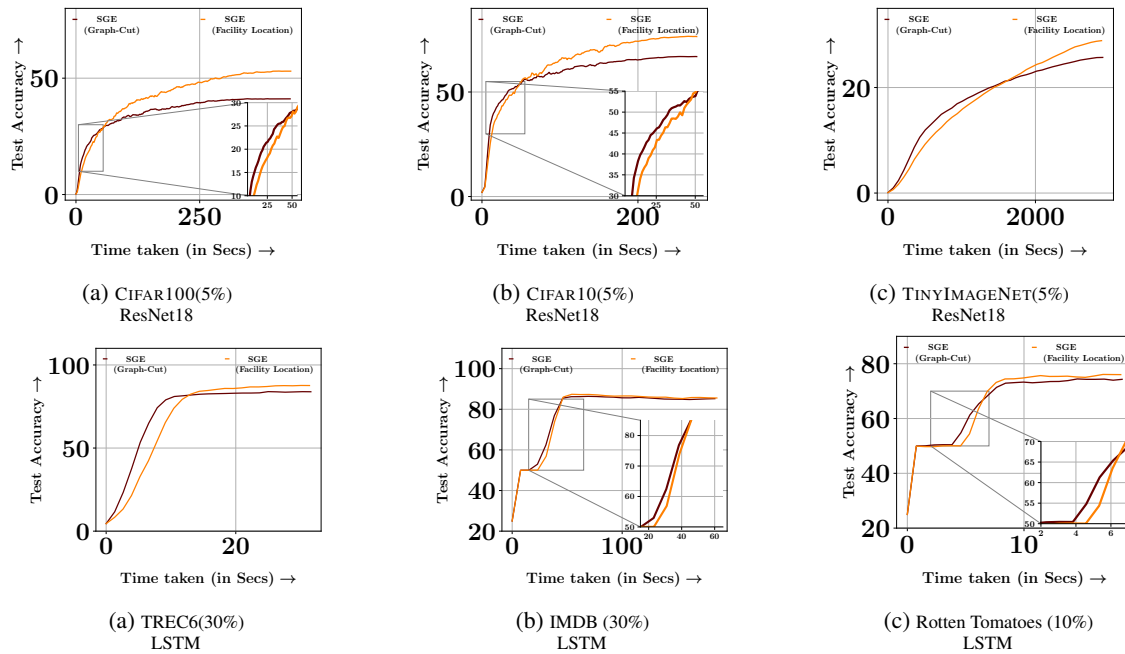


Figure 6: Comparison of initial convergence of SGE with Graph-Cut and SGE with Facility Location on a variety of datasets using different subset sizes. Results show that SGE with Graph-Cut achieves faster initial convergence compared to SGE with Facility Location across all the datasets considered and for different subset sizes.

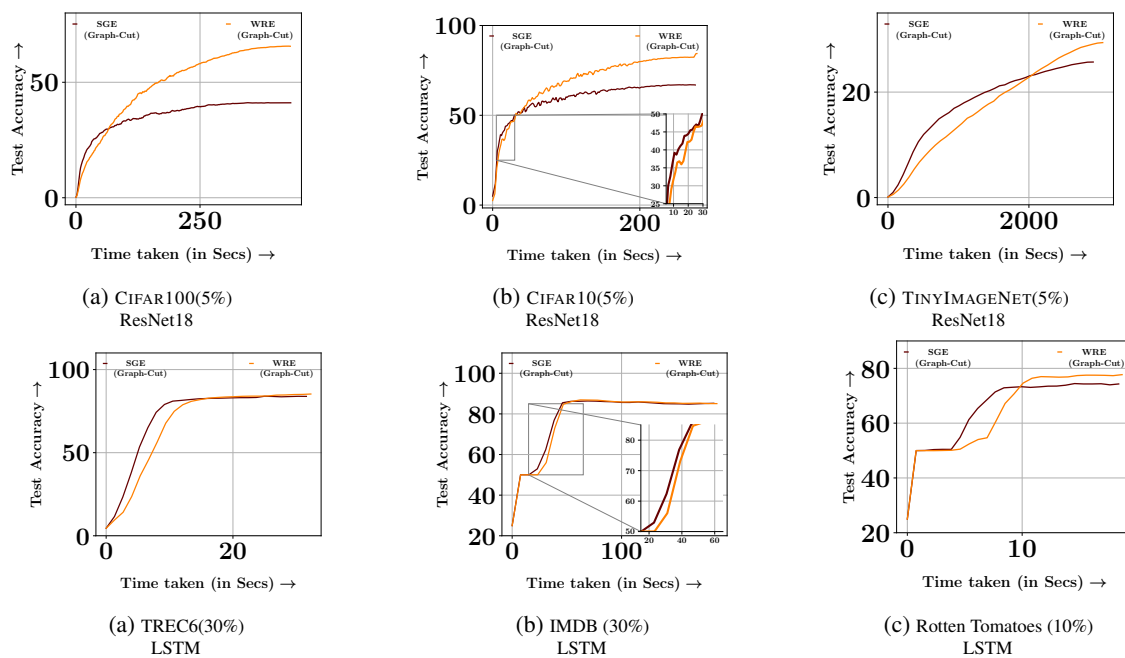


Figure 7: Comparison of initial convergence of SGE with Graph-Cut and WRE with Graph-Cut on a variety of datasets using different subset sizes. Results show that SGE with Graph-Cut achieves faster initial convergence compared to WRE with Graph-Cut across all the datasets considered and for different subset sizes.

### 3.4.3 Developing a Curriculum of Easy-to-Hard Subsets:

Based on the results given in Figures 6, 7 and the empirical success of existing easy-to-hard curriculum learning approaches [36, 16, 68], we aim to develop a curriculum of easy-to-hard subsets by employing SGE with graph cut in initial iterations and WRE with disparity-min in later iterations for model training. We build a curriculum of easy-to-hard samples by training the model for a fraction  $\kappa$  of the total number of epochs using SGE with graph cut function and then using WRE with disparity-min for the rest of the total number of epochs.  $\kappa$  is a hyper-parameter that denotes the fraction of the epochs for which we used stochastic exploration with a graph-cut function. Since WRE using disparity-min ensures that subsets consisting of hard and easy samples are selected (with a greater probability for hard samples), using WRE in later iterations minimizes the catastrophic forgetting of the model on easy samples. In our experiments, we set  $\kappa = \frac{1}{6}$ , which we found optimal after tuning the hyper-parameter  $\kappa$ . We present the  $\kappa$  hyper-parameter tuning results in Appendix 4.6.4. Further, we highlight the advantage of the curriculum-based data exploration in achieving superior model convergence and performance through an ablation study given in Section 4.6.3.

---

#### Algorithm 3 MILO Algorithm

---

**Require:** Train set:  $\mathcal{D}$ ; initial params:  $\theta_0$ ; learning rate:  $\alpha$ ; total epochs:  $T$ ; selection interval:  $R$ ; SGE Fraction:  $\kappa$ ; Training Loss:  $L_T$ , Mini-batch size:  $B$ , Subset size:  $k$

```

1:  $f_1(\mathcal{S}) = \sum_{i \in \mathcal{D}} \sum_{j \in \mathcal{S}} s_{ij} - 0.4 \sum_{i \in \mathcal{S}} \sum_{j \in \mathcal{S}} s_{ij}$  //Initialize Graph-Cut function
2:  $f_2(\mathcal{S}) = \min_{i,j \in \mathcal{S}, i \neq j} (1 - s_{ij})$  //Initialize Disparity-Min function
   *** Check if dataset is pre-processed already ***

3: if is_preprocessed( $\mathcal{D}$ ) then
4:    $\mathcal{S}_0, \mathcal{S}_R, \mathcal{S}_{\kappa T - R}, \mathbf{p} = \text{loadmetadata}(\mathcal{D})$  //Retrieve pre-selected subsets and pre-constructed probability from metadata
5: else
6:    $\mathcal{S}_0, \mathcal{S}_R, \mathcal{S}_{\kappa T - R} = \text{SGE}(f_1, \mathcal{D}, k)$  // Stochastic Greedy Exploration with Graph-Cut
   *** Weighted Random Exploration with Disparity-Min ***
7:    $\mathbf{g} = [g_0, g_1, \dots, g_{|\mathcal{D}|}] = \text{GreedySampleImportance}(f_2, \mathcal{D})$ 
8:    $\mathbf{p} = \left[ \frac{1+g_i+0.5g_i^2}{\sum_{j=1}^{|\mathcal{D}|} 1+g_j+0.5g_j^2} \right]_{i=1}^{|\mathcal{D}|}$ 
9:   storemetadata( $\mathcal{D}, \mathcal{S}_0, \mathcal{S}_R, \mathcal{S}_{\kappa T - R}, \mathbf{p}$ ) // Stored selected subsets and constructed probability as metadata
10: end if
11:  $\mathcal{S} = \mathcal{S}_0$  // Initialize the subset
   *** Model training on representative/easy subsets ***

12: for epochs  $t$  in  $0, \dots, \kappa T - 1$  do
13:   if ( $t \bmod R == 0$ ) then
14:      $\mathcal{S} = \mathcal{S}_t$  // Update the Subset
15:   end if
16:    $\theta_{t+1} = \text{BatchSGD}(\mathcal{S}, \alpha, L_T, B, \text{Epochs} = 1)$ 
17: end for
   *** Model training on diverse/hard subsets ***

18: for epochs  $t$  in  $\kappa T, \dots, T - 1$  do
19:   if ( $(t - \kappa T) \bmod R == 0$ ) then
20:     Sample subset  $\mathcal{S}_t$  from dataset  $\mathcal{D}$  using the probability  $\mathbf{p}$  without replacement
21:      $\mathcal{S} = \mathcal{S}_t$  // Update the Subset
22:   end if
23:    $\theta_{t+1} = \text{BatchSGD}(\mathcal{S}, \alpha, L_T, B, \text{Epochs} = 1)$ 
24: end for

25: Output final model parameters  $\theta_T$ 

```

---

## 3.5 MILO Framework

As discussed earlier, in MILO, the model is trained on a curriculum of subsets spanning from representative to diverse subsets. Figure 3 gives a pictorial representation of the MILO training pipeline. We present a pipeline of hyper-parameter tuning with MILO in Figure 8.

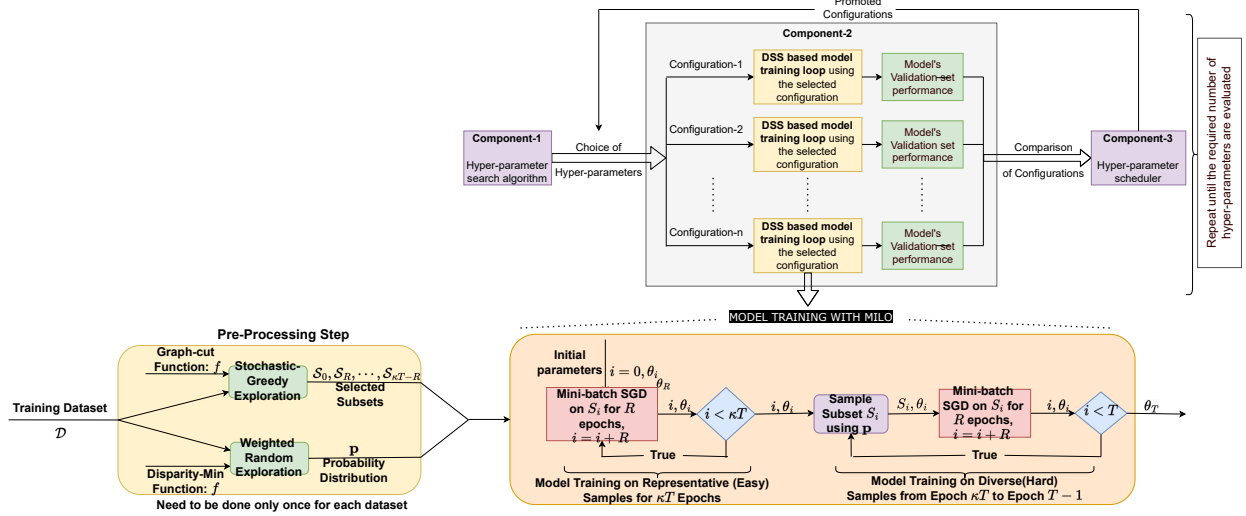


Figure 8: Block Diagram of MILO for hyper-parameter tuning where each individual configuration training is done using MILO instead of training on full dataset.

### 3.5.1 Algorithm and Implementation Aspects

Detailed pseudocode of the MILO algorithm is provided in Algorithm 3. We use Wandb [4] for hyper-parameter search and scheduling algorithms, SUBMODLIB [24] for submodular optimization, and CORDS [26] for baseline subset selection methods.

### 3.5.2 Class-wise Data Partitioning

In this work, all the set functions we experiment with require a similarity kernel  $\mathcal{K}$  of size  $m \times m$ , which must be computed over the entire dataset of size  $m$ . There can be significant increases in memory requirements for computing and storing kernels as the dataset size  $m$  increases making it computationally intractable in some cases. In order to address this problem, we partition the data based on the class labels and select multiple subsets from each class (for SGE) or construct a probability distribution over each class (for WRE) by only considering data instances belonging to each class separately. For example, in the case of a balanced dataset of size  $m$  with  $c$  classes, per-class partitioning allows for a memory requirement reduction by  $c^2$  times. As a default, we use per-class partitioning and curriculum-based data exploration with MILO.

## 4 Experimental Results

Our experiments aim to demonstrate the stability and efficiency of MILO for model training and hyper-parameter tuning. More specifically, we aim at answering the following questions:

**Q1:** Does the proposed MILO approach substantially reduce the training time while maintaining comparable performance to training on the complete dataset?

**Q2:** Can the proposed MILO approach used in conjunction with existing hyper-parameter search and scheduling algorithm achieve faster tuning compared to tuning on the entire dataset?

We repeat each experiment for five runs and report only the mean test accuracies in our plots for better visualization. A detailed table with both mean-test accuracy and the standard deviations are given in Appendix (D.4.1, D.5.2). For a fair comparison, we use the same random seed in each trial for all methods. We explain implementation details, datasets, and baselines used in each scenario in the following subsections.

### 4.1 Subset Selection Baselines

Our experiments aim to demonstrate the effectiveness of MILO for model training and hyper-parameter tuning. **Single Model Training Experiments:** We compare MILO with RANDOM: randomly sample a fixed subset of the same size subset used by MILO from the training data, ADAPTIVE-RANDOM: adaptively sample a random subset of same size

subset used by MILO from the training data every  $R$  epochs, FULL: using the entire training data for model training and tuning, FULL-EARLYSTOP: where we do an early stop to full training to match the time taken (or energy used) by MILO, and adaptive gradient-based subset selection strategies for efficient learning where a new subset is selected every  $R$  epochs, namely CRAIGPB: the faster per-batch version of CRAIG [47] shown in Killamsetty et al. [27], GLISTER [28], GRAD-MATCHPB: the per-batch version of GRAD-MATCH [27]. **Hyper-parameter Tuning Experiments:** We follow the experimental setup of AUTOMATA [30], an efficient hyperparameter tuning framework using GRAD-MATCHPB and replace the subset selection strategy with MILO. Figure 8 gives a pictorial depiction of the hyper-parameter tuning pipeline with MILOAs discussed in AUTOMATA [30], hyper-parameter tuning pipeline contains of three major components: a) hyper-parameter search algorithms - that returns the list of hyper-parameter configurations that needs to be evaluated; b) configuration evaluations involving subset based model training runs - where for each configuration, we train a model using the selected configuration on the subsets selected by MILO , c) hyper-parameter schedulers - that decides the resources allocated for each configuration evaluation and what configurations to be discarded early. We evaluate the effectiveness of MILO for hyperparameter tuning, by performing subset based configuration evaluations using RANDOM, FULL, ADAPTIVE-RANDOM, and AUTOMATA(GRAD-MATCHPB) as subset selection baselines. For tuning with FULL datasets, the entire dataset is used to train the model during hyper-parameter tuning. But for other baselines, we use a subset of the dataset to train various models during tuning.

## 4.2 Datasets, Model Architecture, and Experimental Setup:

We perform experiments on vision and text datasets namely, CIFAR100 (60000 instances) [34], CIFAR10 (60000 instances) [34], TINYIMAGENET (120000 instances) [35], TREC6 [38, 18], IMDB (50000 instances) [45], and ROTTEN TOMATOES (10662 instances) [49]. Whenever the datasets do not have a pre-specified validation set, we split the original training set into a new training set (90%) and a validation set (10%). We give more details on dataset sizes and splits in Appendix D.2. For text datasets, we use the LSTM model (from PyTorch) with trainable GloVe embeddings [52] of dimension 300 as input and the BERT+MLP model consisting of BERT-BASE [11] model with an added two layer MLP for classification. For vision datasets, we use the ResNet18 [17] and ResNet101 [17] models. We train the ResNet [17] models for 200 epochs using a batch size of 128. We train the LSTM model for 24 epochs and the BERT model for 12 epochs using a batch size of 16. For Image datasets, with MILO and baselines, we use Nesterov’s accelerated SGD optimizer with a learning rate of 0.05, weight decay of  $5e-4$ , the momentum of 0.9, and a cosine annealing [43] learning rate scheduler for all the experiments. For text datasets using the LSTM model, we use the Adam optimizer [31] with a learning rate of 0.001. For BERT model finetuning, we use the AdamW optimizer [44] with a learning rate of  $5e-5$ . We present the hyper-parameter search spaces considered for hyper-parameter tuning experiments in Appendix D.3. Finally, all experiments were run on 80GB A100 GPUs.

## 4.3 Pre-trained Transformer Models as Feature Encoders

For vision datasets, we employ the DINO-ViTB16 model [6] available from the HuggingFace [67] as the feature encoder and use the final layer CLS token embedding output as the feature representation. For text datasets, we use the pre-trained all-distilroberta-v1 model available from sentence transformers [57] package and compute the average of the final layer embeddings of all words in the sentence. We present a study evaluating the performance of pre-trained vision transformers and language models as feature encoders for subset selection in Section 4.6.

## 4.4 Efficacy of MILO for Efficient Model Training

The results comparing the accuracy-efficiency tradeoff between the different subset selection approaches for model training are shown in Figure 9. We compare the performance for different subset sizes of the training data: 1%, 5%, 10%, and 30%. Our experiments use a  $R$  value of 1 (i.e., subset selection every epoch) for MILO and ADAPTIVE-RANDOM. We empirically observed that using  $R = 1$  results in better model performance with MILO. We present the ablation study for  $R$  in Appendix 4.6.5. In order to achieve comparable efficiency with other adaptive baselines, including CRAIGPB, GRADMATCHPB, and GLISTER, we use an  $R$  value of 10 for vision experiments and a  $R$  value of 3 for text experiments. Sub-figures(9a, 9b, 9c, 9d, 9e, 9f) show the plots of accuracy degradation vs speedup, both w.r.t full training. From the results, it is evident that MILO achieved the best speedup vs. accuracy tradeoff and is thereby environmentally friendly based on CO2 emissions compared to other baselines. In particular, MILO achieves speedup gains of 3.34x and 10.69x with a performance loss of 1.03% and 4.07% using ResNet18 on CIFAR10. Further, MILO achieves speedup gains of around 3.2x with a performance loss of 1.30% and 3.18% using ResNet101 on TinyImageNet and CIFAR100 datasets. MILO achieves even greater speedup gains of around 10x with a performance loss of 2.30% and 1.23% on TREC6 and Rotten Tomatoes datasets. We also find the MILO is highly effective for finetuning of BERT+MLP model on the IMDB dataset achieving a speedup gain of 24.94x with a performance loss of 1.20%. Another key observation is that ADAPTIVE-RANDOM baseline performs very poorly on text datasets compared to

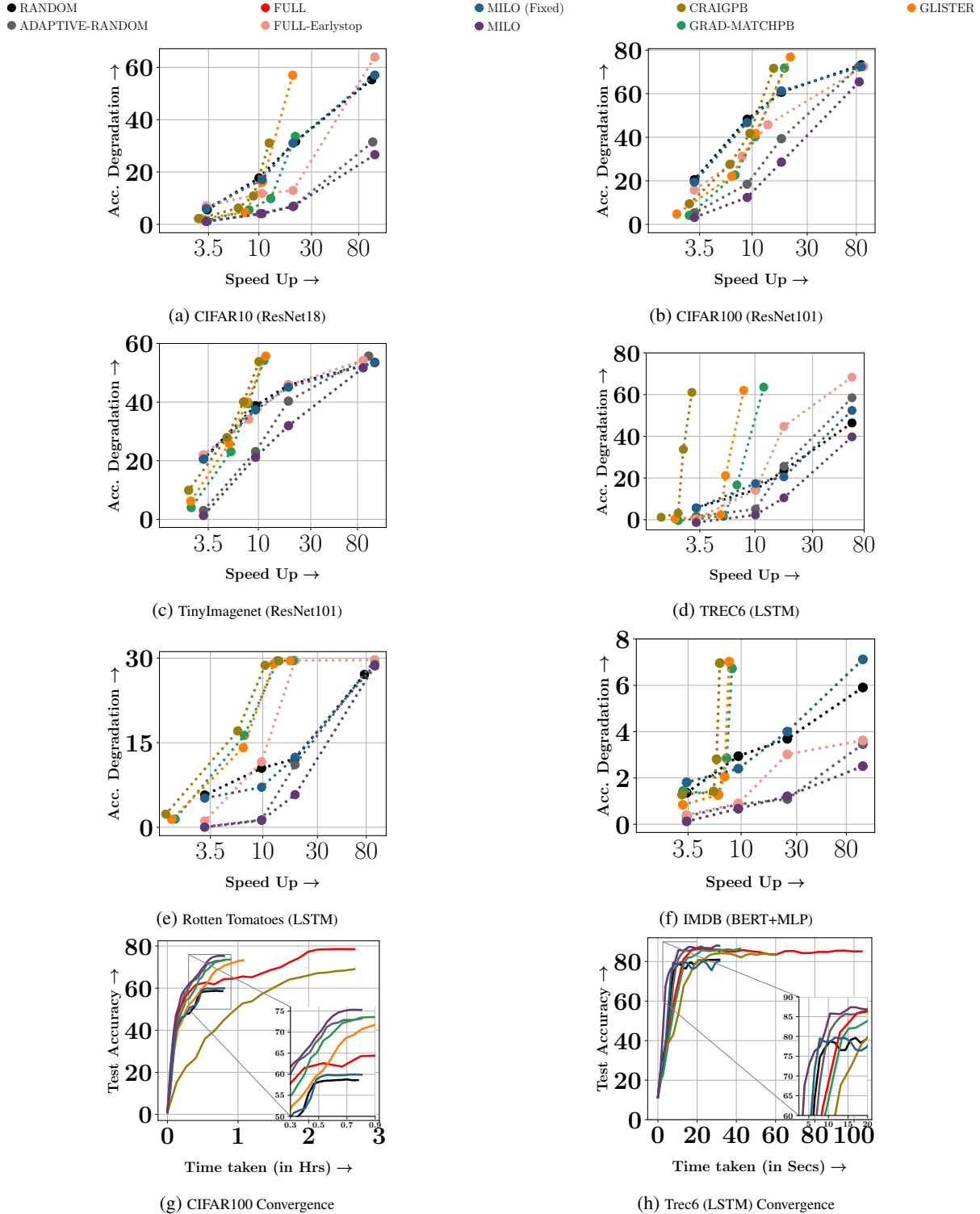


Figure 9: A comparison of MILO with baselines for model training using subset sizes of 1%, 5%, 10%, and 30%. SpeedUp vs Accuracy Degradation, both compared to full data training for (a) ResNet18 on CIFAR-10, (b) ResNet101 on CIFAR100, (c) ResNet101 on TinyImageNet, (d) LSTM on TREC6, (e) LSTM on Rotten Tomatoes, and (f) BERT+MLP on IMDB. On each scatter plot, smaller subsets appear on the right, and larger ones appear on the left. We observe that MILO significantly outperforms existing baselines in terms of accuracy degradation and speedup tradeoff compared to full data training (**bottom-right corner of each plot indicates the best speedup-accuracy tradeoff region**). Plots (g) and (h) show the model convergence with time. *Again, we see that MILO achieves much faster convergence than all baselines and full training.*

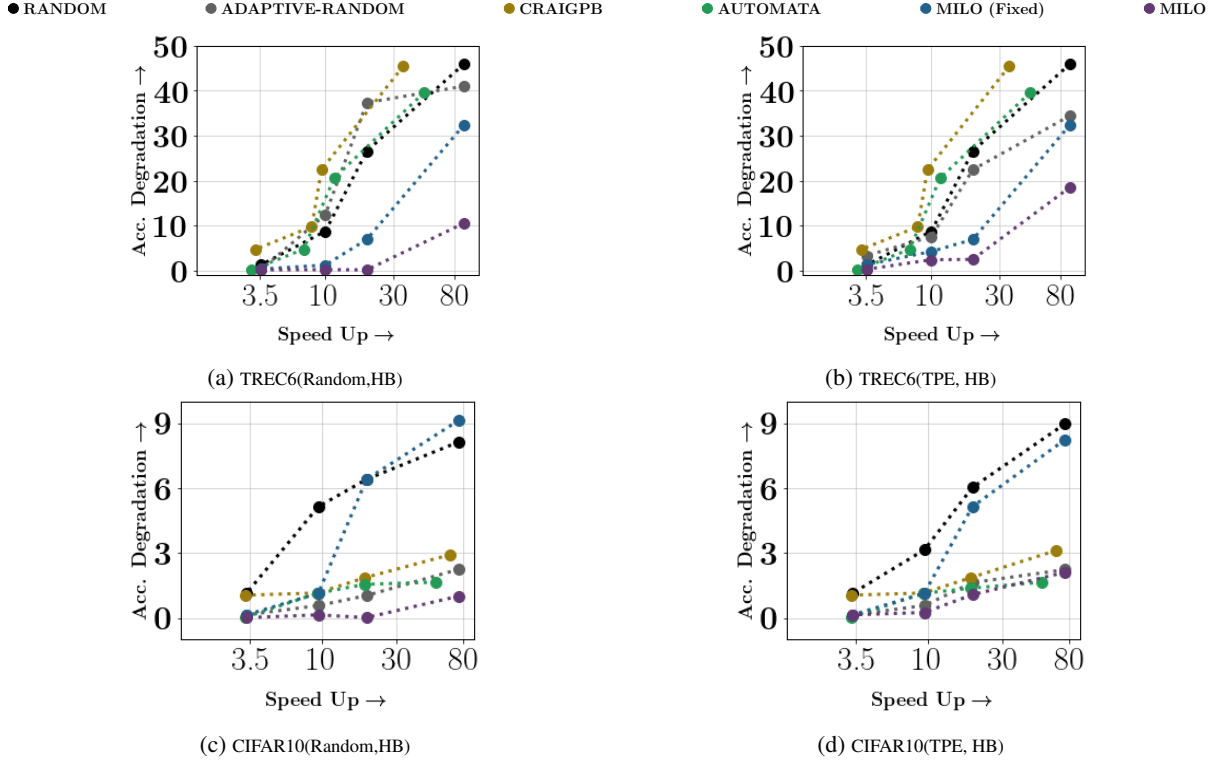


Figure 10: A comparison of MILO with baselines for hyper-parameter tuning using subset sizes of 1%, 5%, 10%, and 30%. In sub-figures (a-d), we present speedup vs. accuracy degradation (in %), compared to Full data tuning for different methods. On each scatter plot, smaller subsets appear on the right, and larger ones appear on the left. Results are shown for (a-b) TREC6, (c-d) CIFAR10 datasets for combinations of a)Random Search and Hyperband Scheduler and b)TPE and Hyperband Scheduler. *The scatter plots show that MILO achieves the best speedup-accuracy tradeoff in almost every case (bottom-right corner of each plot indicates the best speedup-accuracy tradeoff region).*

image datasets. Even on vision datasets, we observe that the effectiveness of ADAPTIVE-RANDOM decreases with the increase of dataset complexity, as evident by the increasing gap between MILO and ADAPTIVE-RANDOM on CIFAR10, CIFAR100, and TinyImagenet datasets. Sub-figures(9g, 9h) show that MILO achieves faster convergence compared to all other methods on CIFAR100 and TREC6 datasets using 30% subsets.

#### 4.5 Efficacy of MILO for Hyper-parameter Tuning

We evaluate the effectiveness of MILO in preserving the original hyper-parameter ordering in Appendix D.5.1. We observe that MILO retains the hyper-parameter ordering better than the baselines. The results comparing the accuracy-efficiency tradeoff between the different subset selection approaches for hyper-parameter tuning are shown in Figure 10. We compare the performance for different subset sizes of the training data: 1%, 5%, 10%, and 30% for combinations of a)Random Search [53] and Hyperband Scheduler [37] and b)TPE [3] and Hyperband Scheduler [37]. Sub-figures(10a, 10b, 10c, 10d) show the plots of accuracy degradation vs. speedup, both w.r.t full data tuning and consistently gives better performance even for small subset sizes, unlike the baselines. From the results, it is evident that MILO achieved the best speedup vs. accuracy tradeoff for hyper-parameter tuning. More specifically, MILO achieves around  $75\times$  speedup on the CIFAR10 dataset with a performance loss of around 0.1%. On the TREC6 dataset, MILO achieves a speed up of around  $20\times$  with a performance loss of around 0.1%.

#### 4.6 Additional Experiments

##### 4.6.1 Performance Comparison of Existing Pre-trained Transformer Models as Feature Encoders

In this study, we evaluate the effectiveness of various existing pre-trained transformer models as feature encoders for subset selection.



(a) Comparison of Vision Transformers for Subset Selection

(b) Comparison of Language Models for Subset Selection

Figure 11: Sub-figure (a) shows the performance of the ResNet18 model trained on a fixed 5% subset of the CIFAR100 dataset selected by maximizing Facility Location function using different pre-trained vision transformer models. Sub-figure (b) shows the performance of the LSTM model trained on a fixed 5% subset of the TREC6 dataset selected by maximizing the Facility Location function using different pre-trained language models.

**Optimal Feature Encoders for Vision Datasets:** For vision datasets, we test with DINO-ViTB16 [6], ViT-LARGE-PATCH16-224-IN21K [12], and CLIP-ViT-L-14 [56] models available from the HuggingFace [67] as the feature encoder. For CLIP model, we use CLIP ViT’s final projection layer output embedding as the feature representation. For both DINO and ViT models, we test with two different types of embeddings as feature vectors: a) we use the final layer CLS token embedding output as the feature representation; b) we use the average of the final layer output embeddings of the constituent patches as the feature representation. We denote the DINO model using CLS token output as feature representation vector by DINO (CLS). Similarly, we denote the ViT model using CLS token output as feature representation vector by ViT (CLS). Sub-figure 11a shows performance of ResNet18 model trained on a fixed 5% subset of the CIFAR100 dataset selected by maximizing the facility location function using different pre-trained vision transformer models as the feature encoder. In this experiment, we used the facility location set function because when using fixed subsets of small subset sizes, facility location yielded optimal results (See Sub-figure 4a). The results presented in Sub-figure 11a indicate that the DINO model using the final layer CLS token embedding as the feature representation gave the best model performance. Hence, in our experiments, we use the DINO model and compute the feature representations for images by using the final layer CLS token output embedding.

**Optimal Feature Encoders for Text Datasets:** For text datasets, we test with ALL-DISTILROBERTA-V1 [40], and ALL-MPNET-BASE-V2 [60] models available from the the Sentence Transformers [57] as the feature encoder. We employ pre-trained models from the Sentence Transformers package, as they have been fine-tuned to produce improved representations that accurately compute the similarity between phrases for natural language inference (NLI) tasks. Similar to the SBERT [57] work, we compute the sentence representations by taking the average of the final layer output embeddings of all the constituent tokens. Sub-figure 11a shows performance of the LSTM model trained on a fixed 5% subset of the TREC6 dataset selected by maximizing the facility location function using different pre-trained language models as the feature encoder. In this experiment, we used the facility location set function because when using fixed subsets of small subset sizes, facility location yielded optimal results (See Sub-figure 4a). Results presented in the Sub-figure 11b shows that ALL-DISTILROBERTA-V1 resulted in better model performance compared to ALL-MPNET-BASE-V2. Hence, in our experiments, we use the ALL-DISTILROBERTA-V1 as the feature encoder for text datasets.

#### 4.6.2 Optimal Similarity Metric Analysis

In this experiment, we aim to analyze the performance of different similarity metrics for computation of similarity between data samples. As part of our experiment, we evaluate the following similarity metrics:

*Cosine Similarity:* Given two data sample  $e_1, e_2$  having feature representations  $r_1, r_2$ , the similarity between the data samples using the cosine-similarity is as follows:

$$\text{Cosine-Similarity}(r_1, r_2) = \frac{r_1 \cdot r_2}{\|r_1\| \|r_2\|} \quad (6)$$

*Dot Product:* Given two data sample  $e_1, e_2$  having feature representations  $r_1, r_2$ , the similarity between the data samples using the dot-product is  $r_1 \cdot r_2$

*RBF Kernel:* Given two data sample  $e_1, e_2$  having feature representations  $r_1, r_2$ , the similarity between the data samples using the RBF kernel is as follows:

$$\text{RBF-Kernel}(r_1, r_2) = \exp\left(-\frac{\|r_1 - r_2\|^2}{kw * \text{mean\_dist}}\right) \quad (7)$$

In the above equation, the parameter  $kw$  is a hyper-parameter that controls the saturation of the similarity between data samples and the parameter  $\text{mean\_dist}$  is the mean-distance of the pair-wise distance between all the samples in the dataset. In the case of small  $kw$  values, the similarity between samples of data drops dramatically with even a small increase in distance between them. In contrast with high  $kw$  values, the similarity between samples of data drops slowly with an increase in distance between them. We also test with different  $kw$  values of 0.01, 0.05, 0.1, 0.5, 1 in this experiment.

**Similarity Metric for Vision Datasets:** Table 1 shows the test accuracies of a ResNet18 model trained on a 5% fixed CIFAR100 subset selected by maximizing the facility location function using the DINO model with final layer CLS token outputs as feature representations using different similarity metrics. Results demonstrate that with DINO model using cosine-similarity resulted in better performing model compared to other similarity metrics. Hence in our work for vision experiments, we use cosine-similarity as the similarity metric. We do not show results with dot-product in Table 1 as the CLS token embedding outputs of the DINO model are normalized because of which both dot-product and cosine similarity give the same similarity values.

Similarity Metric	Test Accuracy
Cosine Similarity	<b>28.68 ± 0.1103</b>
RBF Kernel ( $kw=0.01$ )	27.14 ± 0.2051
RBF Kernel ( $kw=0.05$ )	27.88 ± 0.8132
RBF Kernel ( $kw=0.1$ )	28.11 ± 0.1499
RBF Kernel ( $kw=0.5$ )	27.61 ± 0.601
RBF Kernel ( $kw=0.1$ )	27.62 ± 0.6576

Table 1: Comparison of accuracies of ResNet18 model trained on a 5% fixed CIFAR100 subset selected by maximizing the facility location function using the DINO model with CLS token outputs as feature representations using different similarity metrics.

**Similarity Metric for Text Datasets:** Table 2 shows the test accuracies of the LSTM model trained on a 5% fixed TREC6 subset selected by maximizing the facility location function using the ALL-DISTILROBERTA-V1 as the feature encoder using different similarity metrics. Results demonstrate that with ALL-DISTILROBERTA-V1 model using cosine-similarity resulted in better performing model compared to other similarity metrics. Hence in our work for text experiments, we use cosine-similarity as the similarity metric.

Similarity Metric	Test Accuracy
Cosine Similarity	<b>72.1 ± 2.1508</b>
Dot Product	70.38 ± 4.5514
RBF Kernel ( $kw=0.01$ )	63.58 ± 9.8051
RBF Kernel ( $kw=0.05$ )	67.58 ± 2.561
RBF Kernel ( $kw=0.1$ )	66.92 ± 2.715
RBF Kernel ( $kw=0.5$ )	70.7 ± 2.291
RBF Kernel ( $kw=0.1$ )	70.54 ± 4.518

Table 2: Comparison of accuracies of LSTM model trained on a 5% fixed TREC6 subset selected by maximizing the facility location function using the ALL-DISTILROBERTA-V1 as the feature encoder using different similarity metrics.

#### 4.6.3 Advantages of using a Curriculum for Data Exploration

Results given in Table 3 show that  $\kappa = 0$  (WRE with disparity-min) and  $\kappa = 1$  (SGE with graph-cut) perform poorly compared to using a curriculum  $\kappa > 0$ , thereby proving the efficiency of curriculum-based data exploration over WRE in achieving better performing models. Further, we also showcase the efficiency of curriculum-based data exploration in achieving faster convergence by showing the convergence curves of the ResNet18 model trained on the TINYIMAGENET, CIFAR10 datasets using 5% subsets in Figure 12. The convergence curves show that curriculum-based data exploration converges faster than WRE with disparity-min while achieving better performance than SGE with the graph-cut function.

Tuning of the hyper-parameter: $\kappa$										
Dataset	Model	Graphcut Interval Budget	Mean Test Accuracy of the Model (for 5 runs)							
			0	$\frac{1}{12}$	$\frac{1}{10}$	$\frac{1}{8}$	$\frac{1}{6}$	$\frac{1}{4}$	$\frac{1}{2}$	1
CIFAR100	ResNet101	1%	4.116%	9.27 %	11.795 %	12.135%	<b>12.985%</b>	10.68%	11.11%	3.48%
		5%	45.19%	45.7%	45.43%	47.15%	<b>49.885%</b>	49.01%	48.77%	35.76%
		10%	60.4%	64.08%	64.07%	64.84%	<b>66.11%</b>	64.97%	62.43%	53.41%
		30%	74.28%	74.39%	75.24%	74.27%	<b>75.28%</b>	74.68%	73.18%	71.48%
CIFAR10	ResNet101	1%	38.18%	39.23%	34.61%	38.25%	43.37%	<b>43.92%</b>	38.885%	38.76%
		5%	71.77%	74.13%	77.98%	75.14%	<b>81.63%</b>	77.87%	75.18%	63.9%
		10%	87.21%	85.74%	87.32%	87.96%	<b>88.72%</b>	88.17%	86.61%	83.25%
		30%	93.79%	93.82%	93.52%	93.75%	<b>94.24%</b>	93.73%	93.5%	91.23%

Table 3: Mean test set accuracy of ResNet101 trained on CIFAR10 and CIFAR100 dataset with different subset sizes (of 1%, 5%, 10%, and 30%) and 200 epochs using curriculum-based data exploration with various curriculum intervals.

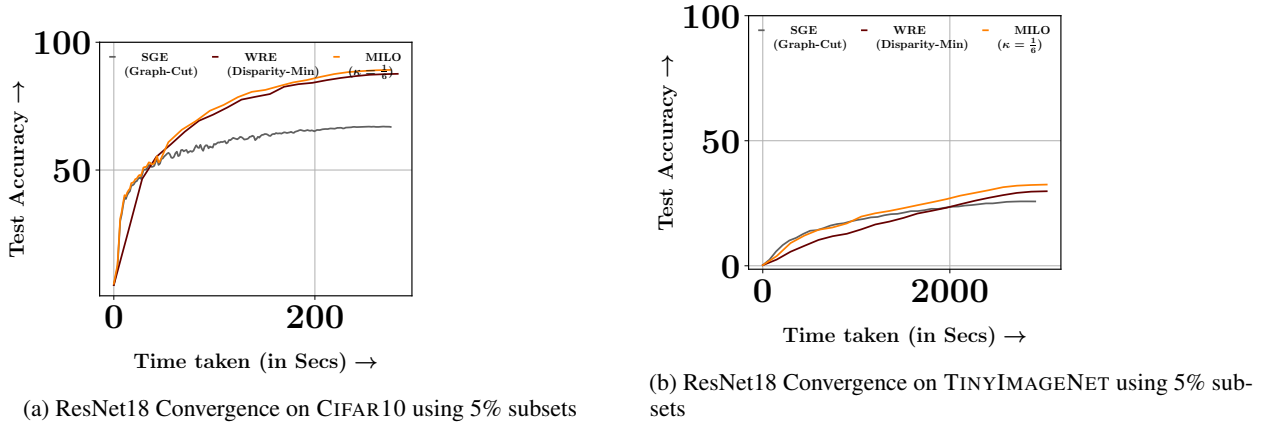


Figure 12: Sub-figure (a) shows the convergence rate of the ResNet18 model on CIFAR10 dataset using 5% subsets selected by SGE with Graph-Cut, WRE with Disparity-Min, and MILO with curriculum exploration. Sub-figure (b) shows the convergence rate of the ResNet18 model on TINYIMAGENET dataset using 5% subsets selected by SGE with Graph-Cut, WRE with Disparity-Min, and MILO with curriculum exploration.

#### 4.6.4 Finding Optimal Curriculum for Data Exploration

In order to find the optimal value of  $\kappa$ , we test for a number of different values that represent the fraction of the total number of epochs for which the model is initially trained using SGE with the graph-cut function. We present the mean test accuracies of the ResNet101 model trained for 200 epochs on different subset sizes of the CIFAR10 and CIFAR100 datasets in Table 3. Based on our observations,  $\kappa = \frac{1}{6}$  is the optimal value and results in higher model accuracy. In Table 3, the results given in column  $\kappa = 0$  correspond to the ResNet101 model trained by simply using WRE with the disparity-min set function without any curriculum. At the same time, using very large values of  $\kappa$  prioritizes more SGE and results in poor performance as SGE is shown to be less effective than WRE based on the results given in Sub-figure 5.

#### 4.6.5 Optimal $R$ analysis

In order to find the optimal  $R$  value ( $R$  signifies how frequently we select a new subset using MILO), we experiment with  $R$  values of [1, 2, 5, 10] on the CIFAR100 dataset using ResNet18 model for subsets sizes of 10%, and 30%. Mean-test accuracy of the ResNet18 model obtained using different  $R$  values is presented in Table 4. Results show that using  $R = 1$ , i.e., selecting a new subset every epoch, results in a better-performing model than using higher values of  $R$ . Further, with small subset sizes, the gap between the model’s performance obtained using  $R = 1$  and other values of  $R$  is even more significant. This shows that it is paramount to select new subsets as frequently as possible when using small subset sizes to achieve the best possible performance. Even though we present test accuracy results for all the ablation studies, we also observe similar patterns with validation accuracies.

Tuning of the hyper-parameter: $R$						
Dataset	Model	R Budget	Mean Test Accuracy of the Model(for 5 runs)			
			1	2	5	10
CIFAR100	ResNet18	10%	<b>69.28% ± 0.1041</b>	69.21% ± 3.82	66.63% ± 3.38	64.07% ± 3.32
		30%	<b>74.95% ± 0.39</b>	74.13% ± 0.36	73.55% ± 0.16	72.72% ± 0.01

Table 4: Mean test set accuracy of ResNet18 trained on CIFAR100 dataset for subset sizes of 10%, and 30% selected using MILO for 200 epochs for different values of  $R$ .

## 5 Conclusion

We introduce MILO, a probabilistic subset selection method for efficient training and tuning. We show that MILO is model-agnostic and is as efficient as random subset selection while achieving superior model convergence compared to existing SOTA subset selection strategies. Empirically, we show that MILO achieves  $3 \times -10 \times$  faster model training and  $20 \times -75 \times$  faster hyper-parameter tuning with minimal performance loss. We believe that MILO contributes significantly to society by allowing faster and more energy-efficient modeling training and tuning, resulting in lower CO2 emissions. However, MILO is reliant on the availability of pre-trained models for feature encoding, which may be a limitation in some specialized domains where pre-trained models are scarce. This limitation, however, is expected to be addressed as a result of ongoing research on training domain-specific and multi-modal transformer architectures.

## References

- [1] Jordan T Ash, Chicheng Zhang, Akshay Krishnamurthy, John Langford, and Alekh Agarwal. Deep batch active learning by diverse, uncertain gradient lower bounds. In *ICLR*, 2020.
- [2] Brian R. Bartoldson, Bhavya Kailkhura, and Davis Blalock. Compute-efficient deep learning: Algorithmic trends and opportunities, 2022. URL <https://arxiv.org/abs/2210.06640>.
- [3] James Bergstra, Rémi Bardenet, Yoshua Bengio, and Balázs Kégl. Algorithms for hyper-parameter optimization. In J. Shawe-Taylor, R. Zemel, P. Bartlett, F. Pereira, and K. Q. Weinberger, editors, *Advances in Neural Information Processing Systems*, volume 24. Curran Associates, Inc., 2011. URL <https://proceedings.neurips.cc/paper/2011/file/86e8f7ab32cfd12577bc2619bc635690-Paper.pdf>.
- [4] Lukas Biewald. Experiment tracking with weights and biases, 2020. URL <https://www.wandb.com/>. Software available from wandb.com.
- [5] Vighnesh Birodkar, Hossein Mobahi, and Samy Bengio. Semantic redundancies in image-classification datasets: The 10% you don’t need. *CoRR*, abs/1901.11409, 2019. URL <http://arxiv.org/abs/1901.11409>.
- [6] Mathilde Caron, Hugo Touvron, Ishan Misra, Hervé Jégou, Julien Mairal, Piotr Bojanowski, and Armand Joulin. Emerging properties in self-supervised vision transformers. *2021 IEEE/CVF International Conference on Computer Vision (ICCV)*, pages 9630–9640, 2021.
- [7] Chih-Chung Chang and Chih-Jen Lin. LIBSVM: A library for support vector machines. *ACM Transactions on Intelligent Systems and Technology*, 2:27:1–27:27, 2011. Software available at <http://www.csie.ntu.edu.tw/~cjlin/libsvm>.
- [8] Cody Coleman, Christopher Yeh, Stephen Mussmann, Baharan Mirzasoleiman, Peter Bailis, Percy Liang, Jure Leskovec, and Matei Zaharia. Selection via proxy: Efficient data selection for deep learning. In *International Conference on Learning Representations*, 2020. URL <https://openreview.net/forum?id=HJg2b0VYDr>.
- [9] Anirban Dasgupta, Ravi Kumar, and Sujith Ravi. Summarization through submodularity and dispersion. In *Proceedings of the 51st Annual Meeting of the Association for Computational Linguistics (Volume 1: Long Papers)*, pages 1014–1022, Sofia, Bulgaria, August 2013. Association for Computational Linguistics. URL <https://aclanthology.org/P13-1100>.
- [10] Alexandre de Brébisson and Pascal Vincent. An exploration of softmax alternatives belonging to the spherical loss family. In Yoshua Bengio and Yann LeCun, editors, *4th International Conference on Learning Representations, ICLR 2016, San Juan, Puerto Rico, May 2-4, 2016, Conference Track Proceedings*, 2016. URL <http://arxiv.org/abs/1511.05042>.
- [11] Jacob Devlin, Ming-Wei Chang, Kenton Lee, and Kristina Toutanova. Bert: Pre-training of deep bidirectional transformers for language understanding. *ArXiv*, abs/1810.04805, 2019.

- [12] Alexey Dosovitskiy, Lucas Beyer, Alexander Kolesnikov, Dirk Weissenborn, Xiaohua Zhai, Thomas Unterthiner, Mostafa Dehghani, Matthias Minderer, Georg Heigold, Sylvain Gelly, Jakob Uszkoreit, and Neil Houlsby. An image is worth 16x16 words: Transformers for image recognition at scale. In *International Conference on Learning Representations*, 2021. URL <https://openreview.net/forum?id=YicbFdNTTy>.
- [13] Pavlos Efraimidis and Paul (Pavlos) Spirakis. *Weighted Random Sampling*, pages 2365–2367. Springer New York, New York, NY, 2016. ISBN 978-1-4939-2864-4. doi: 10.1007/978-1-4939-2864-4\_478. URL [https://doi.org/10.1007/978-1-4939-2864-4\\_478](https://doi.org/10.1007/978-1-4939-2864-4_478).
- [14] Satoru Fujishige. *Submodular functions and optimization*. Elsevier, 2005.
- [15] Alkis Gotovos, Hamed Hassani, and Andreas Krause. Sampling from probabilistic submodular models. In C. Cortes, N. Lawrence, D. Lee, M. Sugiyama, and R. Garnett, editors, *Advances in Neural Information Processing Systems*, volume 28. Curran Associates, Inc., 2015. URL <https://proceedings.neurips.cc/paper/2015/file/160c88652d47d0be60bfbfed25111412-Paper.pdf>.
- [16] Guy Hacohen and Daphna Weinshall. On the power of curriculum learning in training deep networks. In Kamalika Chaudhuri and Ruslan Salakhutdinov, editors, *Proceedings of the 36th International Conference on Machine Learning, ICML 2019, 9-15 June 2019, Long Beach, California, USA*, volume 97 of *Proceedings of Machine Learning Research*, pages 2535–2544. PMLR, 2019. URL <http://proceedings.mlr.press/v97/hacohen19a.html>.
- [17] Kaiming He, X. Zhang, Shaoqing Ren, and Jian Sun. Deep residual learning for image recognition. *2016 IEEE Conference on Computer Vision and Pattern Recognition (CVPR)*, pages 770–778, 2016.
- [18] Eduard Hovy, Laurie Gerber, Ulf Hermjakob, Chin-Yew Lin, and Deepak Ravichandran. Toward semantics-based answer pinpointing. In *Proceedings of the First International Conference on Human Language Technology Research*, 2001. URL <https://www.aclweb.org/anthology/H01-1069>.
- [19] Athresh Karanam, Krishnateja Killamsetty, Harsha Kokel, and Rishabh K Iyer. ORIENT: Submodular mutual information measures for data subset selection under distribution shift. In Alice H. Oh, Alekh Agarwal, Danielle Belgrave, and Kyunghyun Cho, editors, *Advances in Neural Information Processing Systems*, 2022. URL <https://openreview.net/forum?id=mhP6mHgrg1c>.
- [20] Angelos Katharopoulos and François Fleuret. Not all samples are created equal: Deep learning with importance sampling. *arXiv preprint arXiv:1803.00942*, 2018.
- [21] Angelos Katharopoulos and Francois Fleuret. Not all samples are created equal: Deep learning with importance sampling. In Jennifer Dy and Andreas Krause, editors, *Proceedings of the 35th International Conference on Machine Learning*, volume 80 of *Proceedings of Machine Learning Research*, pages 2525–2534. PMLR, 10–15 Jul 2018. URL <https://proceedings.mlr.press/v80/katharopoulos18a.html>.
- [22] Vishal Kaushal, Rishabh Iyer, Suraj Kothawade, Rohan Mahadev, Khoshrav Doctor, and Ganesh Ramakrishnan. Learning from less data: A unified data subset selection and active learning framework for computer vision. In *2019 IEEE Winter Conference on Applications of Computer Vision (WACV)*, pages 1289–1299. IEEE, 2019.
- [23] Vishal Kaushal, Suraj Kothawade, Ganesh Ramakrishnan, Jeff Bilmes, and Rishabh Iyer. Prism: A unified framework of parameterized submodular information measures for targeted data subset selection and summarization. *arXiv preprint arXiv:2103.00128*, 2021.
- [24] Vishal Kaushal, Ganesh Ramakrishnan, and Rishabh Iyer. Submodlib: A submodular optimization library, 2022. URL <https://arxiv.org/abs/2202.10680>.
- [25] Salman Khan, Muzammal Naseer, Munawar Hayat, Syed Waqas Zamir, Fahad Shahbaz Khan, and Mubarak Shah. Transformers in vision: A survey. 54(10s), sep 2022. ISSN 0360-0300. doi: 10.1145/3505244. URL <https://doi.org/10.1145/3505244>.
- [26] Krishnateja Killamsetty, Dheeraj Bhat, Ganesh Ramakrishnan, and Rishabh Iyer. CORDS: COResets and Data Subset selection for Efficient Learning, March 2021. URL <https://github.com/decile-team/cords>.
- [27] Krishnateja Killamsetty, Durga Sivasubramanian, Ganesh Ramakrishnan, Abir De, and Rishabh Iyer. Grad-match: Gradient matching based data subset selection for efficient deep model training. In Marina Meila and Tong Zhang, editors, *Proceedings of the 38th International Conference on Machine Learning*, volume 139 of *Proceedings of Machine Learning Research*, pages 5464–5474. PMLR, 18–24 Jul 2021. URL <https://proceedings.mlr.press/v139/killamsetty21a.html>.
- [28] Krishnateja Killamsetty, Durga Sivasubramanian, Ganesh Ramakrishnan, and Rishabh Iyer. Glist: Generalization based data subset selection for efficient and robust learning. *Proceedings of the AAAI Conference on Artificial Intelligence*, 35(9):8110–8118, May 2021. URL <https://ojs.aaai.org/index.php/AAAI/article/view/16988>.

- [29] Krishnateja Killamsetty, Xujiang Zhao, Feng Chen, and Rishabh K Iyer. RETRIEVE: Coreset selection for efficient and robust semi-supervised learning. In A. Beygelzimer, Y. Dauphin, P. Liang, and J. Wortman Vaughan, editors, *Advances in Neural Information Processing Systems*, 2021. URL <https://openreview.net/forum?id=jSz59N8NvUP>.
- [30] Krishnateja Killamsetty, Guttu Sai Abhishek, Aakriti Lnu, Ganesh Ramakrishnan, Alexandre V. Evfimievski, Lucian Popa, and Rishabh K Iyer. AUTOMATA: Gradient based data subset selection for compute-efficient hyper-parameter tuning. In Alice H. Oh, Alekh Agarwal, Danielle Belgrave, and Kyunghyun Cho, editors, *Advances in Neural Information Processing Systems*, 2022. URL <https://openreview.net/forum?id=ajH17-Pb43A>.
- [31] Diederik P. Kingma and Jimmy Ba. Adam: A method for stochastic optimization. In Yoshua Bengio and Yann LeCun, editors, *3rd International Conference on Learning Representations, ICLR 2015, San Diego, CA, USA, May 7-9, 2015, Conference Track Proceedings*, 2015. URL <http://arxiv.org/abs/1412.6980>.
- [32] Katrin Kirchhoff and Jeff Bilmes. Submodularity for data selection in machine translation. In *Proceedings of the 2014 Conference on Empirical Methods in Natural Language Processing (EMNLP)*, pages 131–141, 2014.
- [33] Suraj Kothawade, Vishal Kaushal, Ganesh Ramakrishnan, Jeff Bilmes, and Rishabh Iyer. Submodular mutual information for targeted data subset selection. *arXiv preprint arXiv:2105.00043*, 2021.
- [34] Alex Krizhevsky. Learning multiple layers of features from tiny images. Technical report, 2009.
- [35] Ya Le and Xuan S. Yang. Tiny imagenet visual recognition challenge. 2015.
- [36] Yong Jae Lee and Kristen Grauman. Learning the easy things first: Self-paced visual category discovery. In *CVPR 2011*, pages 1721–1728, 2011. doi: 10.1109/CVPR.2011.5995523.
- [37] Lisha Li, Kevin Jamieson, Giulia DeSalvo, Afshin Rostamizadeh, and Ameet Talwalkar. Hyperband: A novel bandit-based approach to hyperparameter optimization. *J. Mach. Learn. Res.*, 18(1):6765–6816, jan 2017. ISSN 1532-4435.
- [38] Xin Li and Dan Roth. Learning question classifiers. In *COLING 2002: The 19th International Conference on Computational Linguistics*, 2002. URL <https://www.aclweb.org/anthology/C02-1150>.
- [39] Richard Liaw, Eric Liang, Robert Nishihara, Philipp Moritz, Joseph E Gonzalez, and Ion Stoica. Tune: A research platform for distributed model selection and training. *arXiv preprint arXiv:1807.05118*, 2018.
- [40] Yinhan Liu, Myle Ott, Naman Goyal, Jingfei Du, Mandar Joshi, Danqi Chen, Omer Levy, Mike Lewis, Luke Zettlemoyer, and Veselin Stoyanov. Ro{bert}a: A robustly optimized {bert} pretraining approach, 2020. URL <https://openreview.net/forum?id=SyxS0T4tvS>.
- [41] Yuzong Liu, Rishabh Iyer, Katrin Kirchhoff, and Jeff Bilmes. Switchboard ii and fisver i: High-quality limited-complexity corpora of conversational english speech. In *Sixteenth Annual Conference of the International Speech Communication Association*, 2015.
- [42] Ilya Loshchilov and Frank Hutter. Online batch selection for faster training of neural networks. *arXiv preprint arXiv:1511.06343*, 2015.
- [43] Ilya Loshchilov and Frank Hutter. SGDR: Stochastic gradient descent with warm restarts. In *International Conference on Learning Representations*, 2017. URL <https://openreview.net/forum?id=Skq89Scxx>.
- [44] Ilya Loshchilov and Frank Hutter. Decoupled weight decay regularization. In *International Conference on Learning Representations*, 2019. URL <https://openreview.net/forum?id=Bkg6RiCqY7>.
- [45] Andrew L. Maas, Raymond E. Daly, Peter T. Pham, Dan Huang, Andrew Y. Ng, and Christopher Potts. Learning word vectors for sentiment analysis. In *Proceedings of the 49th Annual Meeting of the Association for Computational Linguistics: Human Language Technologies*, pages 142–150, Portland, Oregon, USA, June 2011. Association for Computational Linguistics. URL <http://www.aclweb.org/anthology/P11-1015>.
- [46] Baharan Mirzasoleiman, Ashwinkumar Badanidiyuru, Amin Karbasi, Jan Vondrák, and Andreas Krause. Lazier than lazy greedy. In *Proceedings of the AAAI Conference on Artificial Intelligence*, volume 29, 2015.
- [47] Baharan Mirzasoleiman, Jeff Bilmes, and Jure Leskovec. Coresets for data-efficient training of machine learning models, 2020.
- [48] George L Nemhauser, Laurence A Wolsey, and Marshall L Fisher. An analysis of approximations for maximizing submodular set functions—i. *Mathematical programming*, 14(1):265–294, 1978.
- [49] Bo Pang and Lillian Lee. Seeing stars: Exploiting class relationships for sentiment categorization with respect to rating scales. In *Proceedings of the ACL*, 2005.
- [50] Adam Paszke, Sam Gross, Francisco Massa, Adam Lerer, James Bradbury, Gregory Chanan, Trevor Killeen, Zeming Lin, Natalia Gimelshein, Luca Antiga, Alban Desmaison, Andreas Kopf, Edward Yang, Zachary DeVito, Martin Raison, Alykhan Tejani, Sasank Chilamkurthy, Benoit Steiner, Lu Fang, Junjie Bai, and Soumith Chintala.

- Pytorch: An imperative style, high-performance deep learning library. In H. Wallach, H. Larochelle, A. Beygelzimer, F. d'Alché-Buc, E. Fox, and R. Garnett, editors, *Advances in Neural Information Processing Systems 32*, pages 8024–8035. Curran Associates, Inc., 2019.
- [51] Mansheej Paul, Surya Ganguli, and Gintare Karolina Dziugaite. Deep learning on a data diet: Finding important examples early in training. In M. Ranzato, A. Beygelzimer, Y. Dauphin, P.S. Liang, and J. Wortman Vaughan, editors, *Advances in Neural Information Processing Systems*, volume 34, pages 20596–20607. Curran Associates, Inc., 2021. URL <https://proceedings.neurips.cc/paper/2021/file/ac56f8fe9eea3e4a365f29f0f1957c55-Paper.pdf>.
- [52] Jeffrey Pennington, Richard Socher, and Christopher Manning. GloVe: Global vectors for word representation. In *Proceedings of the 2014 Conference on Empirical Methods in Natural Language Processing (EMNLP)*, pages 1532–1543, Doha, Qatar, October 2014. Association for Computational Linguistics. doi: 10.3115/v1/D14-1162. URL <https://aclanthology.org/D14-1162>.
- [53] Nicolas Pinto, David Doukhan, James J. DiCarlo, and David D. Cox. A high-throughput screening approach to discovering good forms of biologically inspired visual representation. *PLoS Computational Biology*, 5, 2009.
- [54] Omead Pooladzandi, David Davini, and Baharan Mirzasoleiman. Adaptive second order coresets for data-efficient machine learning. In Kamalika Chaudhuri, Stefanie Jegelka, Le Song, Csaba Szepesvari, Gang Niu, and Sivan Sabato, editors, *Proceedings of the 39th International Conference on Machine Learning*, volume 162 of *Proceedings of Machine Learning Research*, pages 17848–17869. PMLR, 17–23 Jul 2022. URL <https://proceedings.mlr.press/v162/pooladzandi22a.html>.
- [55] Xipeng Qiu, Tianxiang Sun, Yige Xu, Yunfan Shao, Ning Dai, and Xuanjing Huang. Pre-trained models for natural language processing: A survey. *CoRR*, abs/2003.08271, 2020. URL <https://arxiv.org/abs/2003.08271>.
- [56] Alec Radford, Jong Wook Kim, Chris Hallacy, Aditya Ramesh, Gabriel Goh, Sandhini Agarwal, Girish Sastry, Amanda Askell, Pamela Mishkin, Jack Clark, Gretchen Krueger, and Ilya Sutskever. Learning transferable visual models from natural language supervision. In Marina Meila and Tong Zhang, editors, *Proceedings of the 38th International Conference on Machine Learning*, volume 139 of *Proceedings of Machine Learning Research*, pages 8748–8763. PMLR, 18–24 Jul 2021. URL <https://proceedings.mlr.press/v139/radford21a.html>.
- [57] Nils Reimers and Iryna Gurevych. Sentence-bert: Sentence embeddings using siamese bert-networks. In *Proceedings of the 2019 Conference on Empirical Methods in Natural Language Processing*. Association for Computational Linguistics, 11 2019. URL <http://arxiv.org/abs/1908.10084>.
- [58] Roy Schwartz, Jesse Dodge, Noah Smith, and Oren Etzioni. Green ai. *Communications of the ACM*, 63:54 – 63, 2020.
- [59] Ozan Sener and Silvio Savarese. Active learning for convolutional neural networks: A core-set approach. In *International Conference on Learning Representations*, 2018.
- [60] Kaitao Song, Xu Tan, Tao Qin, Jianfeng Lu, and Tie-Yan Liu. MpNet: Masked and permuted pre-training for language understanding. In *Proceedings of the 34th International Conference on Neural Information Processing Systems, NIPS’20*, Red Hook, NY, USA, 2020. Curran Associates Inc. ISBN 9781713829546.
- [61] Ben Sorscher, Robert Geirhos, Shashank Shekhar, Surya Ganguli, and Ari S. Morcos. Beyond neural scaling laws: beating power law scaling via data pruning. In Alice H. Oh, Alekh Agarwal, Danielle Belgrave, and Kyunghyun Cho, editors, *Advances in Neural Information Processing Systems*, 2022. URL <https://openreview.net/forum?id=UmvSIP-PyV>.
- [62] Emma Strubell, Ananya Ganesh, and Andrew McCallum. Energy and policy considerations for deep learning in NLP. In *Proceedings of the 57th Annual Meeting of the Association for Computational Linguistics*, pages 3645–3650, Florence, Italy, July 2019. Association for Computational Linguistics. doi: 10.18653/v1/P19-1355. URL <https://aclanthology.org/P19-1355>.
- [63] Rishabh Tiwari, Krishnateja Killamsetty, Rishabh K. Iyer, and Pradeep Shenoy. Gcr: Gradient coreset based replay buffer selection for continual learning. *2022 IEEE/CVF Conference on Computer Vision and Pattern Recognition (CVPR)*, pages 99–108, 2021.
- [64] Mariya Toneva, Alessandro Sordani, Remi Tachet des Combes, Adam Trischler, Yoshua Bengio, and Geoffrey J. Gordon. An empirical study of example forgetting during deep neural network learning. In *International Conference on Learning Representations*, 2019. URL <https://openreview.net/forum?id=BJlxm30cKm>.
- [65] Kai Wei, Yuzong Liu, Katrin Kirchhoff, Chris Bartels, and Jeff Bilmes. Submodular subset selection for large-scale speech training data. In *2014 IEEE International Conference on Acoustics, Speech and Signal Processing (ICASSP)*, pages 3311–3315. IEEE, 2014.

- [66] Kai Wei, Yuzong Liu, Katrin Kirchhoff, and Jeff Bilmes. Unsupervised submodular subset selection for speech data. In *2014 IEEE International Conference on Acoustics, Speech and Signal Processing (ICASSP)*, pages 4107–4111. IEEE, 2014.
- [67] Thomas Wolf, Lysandre Debut, Victor Sanh, Julien Chaumond, Clement Delangue, Anthony Moi, Pierric Cistac, Tim Rault, Rémi Louf, Morgan Funtowicz, Joe Davison, Sam Shleifer, Patrick von Platen, Clara Ma, Yacine Jernite, Julien Plu, Canwen Xu, Teven Le Scao, Sylvain Gugger, Mariama Drame, Quentin Lhoest, and Alexander M. Rush. Huggingface’s transformers: State-of-the-art natural language processing, 2019. URL <https://arxiv.org/abs/1910.03771>.
- [68] Tianyi Zhou, Shengjie Wang, and Jeffrey Bilmes. Curriculum learning by dynamic instance hardness. In H. Larochelle, M. Ranzato, R. Hadsell, M.F. Balcan, and H. Lin, editors, *Advances in Neural Information Processing Systems*, volume 33, pages 8602–8613. Curran Associates, Inc., 2020. URL <https://proceedings.neurips.cc/paper/2020/file/62000dee5a05a6a71de3a6127a68778a-Paper.pdf>.

# Supplementary Material

## Appendix

### Table of Contents

---

<b>A</b>	<b>Code</b>	<b>23</b>
<b>B</b>	<b>Licenses</b>	<b>23</b>
<b>C</b>	<b>Instantiations of Different Submodular Functions</b>	<b>23</b>
C.1	Representation Functions . . . . .	23
C.2	Diversity Functions . . . . .	23
<b>D</b>	<b>More Experimental Details and Additional Results</b>	<b>24</b>
D.1	GPU Resources . . . . .	24
D.2	Additional Datasets Details . . . . .	24
D.3	Additional Experimental Details . . . . .	25
D.4	Additional Model Training Results . . . . .	26
D.5	Additional Hyper-parameter Tuning Results . . . . .	26

---

## A Code

The code of MILO is available at the following link: <https://anonymous.4open.science/r/MILO-282B/>.

## B Licenses

We release the code repository of MILO with MIT license, and it is available for everybody to use freely. We use the popular deep learning framework [50] for implementation of MILO framework, wandb [4] for hyper-parameter search and scheduling algorithms, SUBMODLIB [24] for submodular functions and submodular maximization, and CORDS [26] for subset selection strategies. We use TREC6 [38, 18], IMDB [45], Rotten Tomatoes [49], CIFAR10 [34], CIFAR100 [34], and TINYIMAGENET [35] datasets. IMDB [45] dataset is released with a Non-Commercial License. The license of the TREC6 [38, 18] dataset is CC0:Public Domain [7]. CIFAR10, CIFAR100, and TINYIMAGENET datasets are released with an MIT license. Furthermore, all the datasets and pre-trained models used in this work are publicly available. In addition, the datasets used do not contain any personally identifiable information.

## C Instantiations of Different Submodular Functions

### C.1 Representation Functions

#### C.1.1 Facility Location

Given, a dataset  $\mathcal{D} = \{(x_i, y_i)\}_{i=1}^n$  with n data samples, the facility location objective can be given as following:

$$f(\mathcal{S}) = \sum_{i \in \mathcal{D}} \max_{j \in \mathcal{S}} s_{ij} \quad (8)$$

where  $s_{ij}$  denotes the similarity of data samples  $i$  and  $j$ . For each data point  $i$  in the ground set  $\mathcal{D}$ , we compute the most representative samples  $j$  from subset  $\mathcal{S}$  which is closest to it and add these similarities for all data points. Note that due to the sum-max formulation involved in facility location, having one representative data sample from each cluster in your dataset is enough for maximizing the facility location value. This further prevents the selection of more samples in the subset from more dense regions.

#### C.1.2 Graph-Cut

Given, a dataset  $\mathcal{D} = \{(x_i, y_i)\}_{i=1}^n$  with n data samples, the graph-cut objective can be given as following:

$$f(\mathcal{S}) = \sum_{i \in \mathcal{D}} \sum_{j \in \mathcal{S}} s_{ij} - \lambda \sum_{i \in \mathcal{S}} \sum_{j \in \mathcal{S}} s_{ij} \quad (9)$$

The  $\lambda$  parameter in the above equation controls the trade-off between diversity and representation. When  $\lambda$  is large, the graph cut function also incorporates diversity into its model. In our experiments, we set  $\lambda = 0.4$ , thereby making the graph-cut function model more representation and making it monotone-submodular. Note that due to the sum-sum formulation involved in graph-cut, selection of more samples from dense regions in the center leads to maximization of graph-cut function value. Thus, graph-cut can result in the selection of subsets consisting of easy samples from very dense regions in the dataset.

### C.2 Diversity Functions

#### C.2.1 Disparity-Sum

Given, a dataset  $\mathcal{D} = \{(x_i, y_i)\}_{i=1}^n$  with n data samples, the disparity-sum objective can be given as following:

$$f(\mathcal{S}) = \sum_{i \in \mathcal{S}} \sum_{j \in \mathcal{S}} (1 - s_{ij}) \quad (10)$$

Note that in the above equation, disparity-sum purely concentrates on selected samples that are maximally different from each other in the dataset without any care for the representation.

### C.2.2 Disparity-Min

Given, a dataset  $\mathcal{D} = \{(x_i, y_i)\}_{i=1}^n$  with  $n$  data samples, the disparity-min objective can be given as following:

$$f(\mathcal{S}) = \min_{i,j \in \mathcal{S}, i \neq j} (1 - s_{ij}) \quad (11)$$

In the above equation,  $1 - s_{ij}$  can be considered as a distance measure and maximization of the disparity-min objective results in maximization of minimum distance between the samples in the selected subset. Even though disparity-min objective is not submodular, it is proven to perform empirically well using conventional greedy approaches [9].

## D More Experimental Details and Additional Results

### D.1 GPU Resources

We performed experiments on an 80GB A100 GPU cluster. To be fair in timing computation, we ran MILO and all other baselines for a particular setting on the same GPU server.

### D.2 Additional Datasets Details

#### D.2.1 Text Datasets

We performed experiments on TREC6 [38, 18], IMDB [45], and Rotten Tomatoes [49] text datasets. TREC6 [38, 18] is a dataset for question classification consisting of open-domain, fact-based questions divided into broad semantic categories (ABBR - Abbreviation, DESC - Description and abstract concepts, ENTY - Entities, HUM - Human beings, LOC - Locations, NYM - Numeric values). IMDB and Rotten Tomatoes datasets are sentiment classification datasets based on IMDB and Rotten Tomatoes movie reviews, respectively. Validation data for TREC6 [38, 18] and IMDB [45] datasets are obtained using 10% of the train data. A seed value of 42 is used in the generator argument in the `random_split` function of PyTorch. In Table 5, we summarize the number of classes and number of instances in each split of the text datasets.

Dataset	#Classes	#Train	#Validation	#Test
TREC6	6	4907	545	500
IMDB	2	22500	25000	25000
Rotten Tomatoes	2	8530	1066	1066

Table 5: Number of classes, Number of instances in Train, Validation and Test split in Text datasets

#### D.2.2 Vision Datasets

We performed experiments on CIFAR10 [34], CIFAR100 [34], and TINYIMAGENET [35] datasets. The CIFAR10 [34] dataset contains 60,000 colored images of size  $32 \times 32$  divided into ten classes, each with 6000 images. CIFAR100 [34] is also of size  $32 \times 32$  but contains 600 images per class and 100 classes. Both CIFAR10 [34] and CIFAR100 [34] have 50,000 training samples and 10,000 test samples distributed equally across all classes. TINYIMAGENET [35] dataset contains 120,000 colored images of size  $64 \times 64$  from 200 classes with 600 images per each class.

For both CIFAR10 and CIFAR100 datasets, 10% of the training data is used for validation (seed value = 42). In Table 6, we summarize the number of classes and the number of instances in each split in the image datasets.

Dataset	#Classes	#Train	#Validation	#Test
CIFAR10	10	45000	5000	10000
CIFAR100	100	45000	5000	10000
TINYIMAGENET	200	100000	10000	10000

Table 6: Number of classes, Number of instances in Train, Validation and Test split in Image datasets

### D.3 Additional Experimental Details

#### D.3.1 Model Training Experiments

We compare MILO with RANDOM: randomly sample a fixed subset of the same size subset used by MILO from the training data, ADAPTIVE-RANDOM: adaptively sample a random subset of same size subset used by MILO from the training data every  $R$  epochs, FULL: using the entire training data for model training and tuning, FULL-EARLYSTOP: where we do an early stop to full training to match the time taken (or energy used) by MILO, and adaptive gradient-based subset selection strategies for efficient learning where a new subset is selected every  $R$  epochs, namely CRAIGPB: the faster per-batch version of CRAIG [47] shown in Killamsetty et al. [27], GLISTER [28], GRAD-MATCHPB: the per-batch version of GRAD-MATCH [27]. Our experiments use a  $R$  value of 1 (i.e., subset selection every epoch) for MILO and ADAPTIVE-RANDOM. We empirically observed that using  $R = 1$  results in better model performance with MILO. In order to achieve comparable efficiency with other adaptive baselines, including CRAIGPB, GRADMATCHPB, and GLISTER, we use an  $R$  value of 10 for vision experiments and a  $R$  value of 3 for text experiments.

**Details of Text Experiments** For text datasets, we use the LSTM model (from PyTorch) with trainable GloVe embeddings [52] of dimension 300 as input and the BERT+MLP model consisting of BERT-BASE [11] model with a added two layer MLP for classification. We train the LSTM model for 24 epochs and the BERT model for 12 epochs using a batch size of 16. For text datasets using LSTM model, we use the Adam optimizer [31] with a learning rate of 0.001. For BERT model finetuning, we use the AdamW optimizer [44] with a learning rate of  $5e-5$ .

**Details of Image Experiments** For vision datasets, we use the ResNet18 [17] and ResNet101 [17] models. We train the ResNet [17] models for 200 epochs using a batch size of 128. For training ResNet models with MILO and baselines, we use the Nesterov’s accelerated SGD optimizer with a learning rate of 0.05, weight decay of  $5e-4$ , momentum of 0.9, and a cosine annealing [43] learning rate scheduler for all the experiments.

#### D.3.2 Hyper-Parameter Tuning Experiments

We follow the experimental setup of AUTOMATA [30], an efficient hyperparameter tuning framework using GRAD-MATCHPB and replace the subset selection strategy with MILO. Figure 8 gives a pictorial depiction of the hyper-parameter tuning pipeline with MILO. As discussed in AUTOMATA [30], hyper-parameter tuning pipeline contains of three major components: a) hyper-parameter search algorithms - that returns the list of hyper-parameter configurations that needs to be evaluated; b) configuration evaluations involving subset based model training runs - where for each configuration, we train a model using the selected configuration on the subsets selected by MILO, c) hyper-parameter schedulers - that decides the resources allocated for each configuration evaluation and what configurations to be discarded early. We evaluate the effectiveness of MILO for hyperparameter tuning, by performing subset based configuration evaluations using RANDOM, FULL, ADAPTIVE-RANDOM, and AUTOMATA (GRAD-MATCHPB) as subset selection baselines. For tuning with FULL datasets, the entire dataset is used to train the model during hyper-parameter tuning. But for other baselines, we use a subset of the dataset to train various models during tuning. In addition, the subset selection techniques used are adaptive, which means that the model is trained on a different subset every few epochs. We empirically observed that using  $R = 1$  results in better model performance with MILO. In order to achieve comparable efficiency with other adaptive baselines, including CRAIGPB, and GRADMATCHPB, we use an  $R$  value of 10 for vision experiments and a  $R$  value of 3 for text experiments. We experiment with the combination of a) Random Search [53] and Hyperband [37] scheduler; and b) TPE Search [3] and Hyperband [37]. We only test with Hyperband [37] scheduler because we use Wandb [4] for running hyper-parameter optimization algorithms, and wandb provides the support for Hyperband [37] only. We use Wand for hyper-parameter to accurately compute the tuning times, which we found difficult with Ray [39] due to its high internal communication times.

**Details of Text Experiments** For text datasets, we use the LSTM model (from PyTorch) with trainable GloVe embeddings [52] of dimension 300 as input. The hyper-parameter space for experiments on text datasets include learning rate, hidden size & number of layers of LSTM and batch size of training. Some experiments (with TPE search algorithm) where the best configuration among 108 configurations are found, the hyper-parameter space is learning rate: [0.001,0.1], LSTM hidden size: {64,128,256, 512}, number of layers in LSTM: {1, 2}, batch size: {16,32,64}.

**Details of Image Experiments** For vision datasets, we use the ResNet18 [17] model. The hyper-parameter search space for tuning experiments on image datasets include a choice between Momentum method and Nesterov Accelerated Gradient method, choice of learning rate scheduler and their corresponding parameters, and four different group-wise learning rates,  $lr_1$  for layers of the first group,  $lr_2$  for layers of intermediate groups,  $lr_3$  for layers of the last group of ResNet model, and  $lr_4$  for the final fully connected layer. For learning rate scheduler, we change the learning rates during training using either a cosine annealing schedule or decay it linearly by  $\gamma$  after every 20 epochs. Best configuration for most experiments is selected from 108 configurations where the hyper-parameter space is  $lr_1$ : [0.001,

0.01],  $lr_2$ : [0.001, 0.01],  $lr_3$ : [0.001, 0.01],  $lr_4$ : [0.001, 0.01], Nesterov: {True, False}, learning rate scheduler: {Cosine Annealing, Linear Decay},  $\gamma$ : [0.05, 0.5].

## D.4 Additional Model Training Results

### D.4.1 Test-Accuracies, Training times and Standard deviations

Table 7, Table 9 shows the top-1 test accuracies and training times taken by MILO and the other baselines considered for single model training on CIFAR10, CIFAR100, TINYIMAGENET, TREC6, IMDB, Rotten Tomatoes datasets for different subset sizes of 1%, 5%, 10%, and 30% respectively. Furthermore, Table 8, Table 10 gives the standard deviation numbers of MILO and other baselines for single model training on CIFAR10, CIFAR100, TINYIMAGENET, TREC6, IMDB, Rotten Tomatoes datasets for different subset sizes of 1%, 5%, 10%, and 30% respectively.

## D.5 Additional Hyper-parameter Tuning Results

### D.5.1 Hyper-parameter Ordering Retention Analysis

We evaluate the effectiveness of MILO and the considered subset selection baselines in preserving original hyper-parameter ordering by full data tuning. In a nutshell, we are trying to determine whether the original order of the hyper-parameters is maintained, despite using small subsets for model training runs involved in hyper-parameter tuning. To examine this, we experiment on the Trec6 [38, 18] dataset using an LSTM model. Hyper-parameter search for the TREC6 dataset includes a grid search over 108 configurations of the learning rate, optimizer, LSTM hidden size, training batch size, and the number of final fully connected layers. Table 11 shows the Kendall Tau correlation values between the hyper-parameter ordering obtained using 1%, 5%, and 10% subsets selected by MILO, RANDOM, ADAPTIVE-RANDOM, AUTOMATA, and CRAIGPB and Full data hyper-parameter ordering on TREC6 [38, 18] dataset. Results in Table 11 demonstrate that MILO is more effective than the baselines considered in preserving hyper-parameter ordering even when using small subsets.

### D.5.2 Test-Accuracies, Training times and Standard deviations

Table 12 shows the top-1 test accuracies and tuning times taken by MILO and the other baselines considered for single model training on CIFAR10, TREC6 datasets for different subset sizes of 1%, 5%, 10%, and 30% respectively.

Model Training Results on Vision Datasets														
Dataset	Model	Budget(%)	Top-1 Test accuracy of the Model(%)				Model Training time(in hrs)							
			1%	5%	10%	30%	1%	5%	10%	30%				
CIFAR10	ResNet18	Selection Strategy	FULL (skyline for test accuracy)	95.19	95.19	95.19	95.19	1.72736889	1.72736889	1.72736889	1.72736889	1.72736889	1.72736889	
			RANDOM (skyline for training time)	39.91	63.52	77.47	89.62	0.01646028	0.08030361	0.17222375	0.50628667			
			ADAPTIVE-RANDOM (skyline for training time)	63.71	88.2	91.09	94.05	0.01632191	0.08136123	0.1776311	0.5068371			
		MLO	GLISTER	38.2	79.02	90.67	93.04	0.08538972	0.16018167	0.23015611	0.57614889			
			CRAIGPB	64.11	84.35	88.97	92.99	0.13940694	0.19342472	0.26544833	0.60756111			
			GRADMATCHPB	61.59	85.34	89.67	93.71	0.08093056	0.13492361	0.21210222	0.52081639			
			MILO (Fixed)	38.17	64.17	78.06	89.21	0.01667131	0.0821212	0.172141	0.50281731			
			MILO	68.56	88.37	91.11	94.12	0.0163121	0.08083317	0.1702131	0.50645219			
			FULL (skyline for test accuracy)	31.49	54.35	69.99	88.51	0.02820806	0.14013056	0.27079694	0.85268889			
			RANDOM (skyline for training time)	21.72	80.25	88.13	94.2	0.02720875	0.13807778	0.2795975	0.82271222			
ADAPTIVE-RANDOM (skyline for training time)	10.46	62.41	83.79	92.47	0.12346444	0.24328889	0.38844556	1.05459139						
CIFAR100	ResNet18	Selection Strategy	FULL (skyline for test accuracy)	77.03	77.03	77.03	77.03	1.52	1.52	1.52	1.52	1.52	1.52	
			RANDOM (skyline for training time)	8.937	21.74	35.03	61.93	0.0152	0.0836	0.1554	0.449			
			ADAPTIVE-RANDOM (skyline for training time)	29.99	61.86	69.14	74.82	0.016	0.0757	0.1532	0.4491			
		MLO	GLISTER	2.72	52.17	65.72	72.59	0.0872	0.1553	0.2362	0.5717			
			CRAIGPB	23.38	51.56	59.6	70.25	0.1344	0.193	0.2679	0.5668			
			GRADMATCHPB	24.4	54.42	65.93	73.57	0.07873	0.1384	0.2125	0.4876			
			MILO (Fixed)	9.133	22.57	36.03	61.97	0.13171083	0.23819667	0.41062028	0.9307625			
			MILO	35.34	64.4	69.28	74.95	0.0269	0.1321025	0.28677639	0.850435			
			FULL (skyline for test accuracy)	77.03	77.03	77.03	77.03	1.52	1.52	1.52	1.52			
			RANDOM (skyline for training time)	8.937	21.74	35.03	61.93	0.0152	0.0836	0.1554	0.449			
ADAPTIVE-RANDOM (skyline for training time)	29.99	61.86	69.14	74.82	0.016	0.0757	0.1532	0.4491						
TinyImageNet	ResNet18	Selection Strategy	FULL (skyline for test accuracy)	78.46	78.46	78.46	78.46	2.6034	2.6034	2.6034	2.6034	2.6034	2.6034	
			RANDOM (skyline for training time)	5.18	17.81	30.17	57.93	0.02952	0.14524	0.2879	0.825375			
			ADAPTIVE-RANDOM (skyline for training time)	6.199	39.11	60.02	73.21	0.03112	0.14523	0.2879	0.825175			
		MLO	GLISTER	1.634	36.76	56.37	73.7	0.12156	0.24377	0.39149	1.17212			
			CRAIGPB	6.8	36.68	50.92	69.02	0.1697	0.2727	0.40612	0.912357			
			GRADMATCHPB	6.653	38.23	55.82	74.35	0.136	0.246	0.3665	0.91235			
			MILO (Fixed)	6.064	17.17	31.73	59.05	0.02952	0.14523	0.2879	0.82537			
			MILO	12.99	49.89	66.11	75.28	0.030778	0.145234	0.2879	0.8253			
			FULL (skyline for test accuracy)	52.44	52.44	52.44	52.44	15.411	15.411	15.411	15.411			
			RANDOM (skyline for training time)	3.21	13	19.61	35.68	0.171	0.874	1.82	4.99			
ADAPTIVE-RANDOM (skyline for training time)	0.62	27.34	38.73	50.3	0.168	0.832	1.82	5.12						
TinyImageNet	ResNet101	Selection Strategy	FULL (skyline for test accuracy)	56.32	56.32	56.32	56.32	17.2387	17.2387	17.2387	17.2387	17.2387	17.2387	
			RANDOM (skyline for training time)	2.84	10.52	17.57	35.68	0.150245	0.91737	1.826483	5.437941			
			ADAPTIVE-RANDOM (skyline for training time)	0.6067	15.99	33.19	53.3	0.1710	0.91737	1.82648	5.43794			
		MLO	GLISTER	0.6255	16.3	30.47	50.11	1.47556	2.18824	3.17468	7.099			
			CRAIGPB	2.54	16.23	28.43	46.42	1.7016	2.348	3.32867	7.42342			
			GRADMATCHPB	2.15	16.84	33.25	52.31	1.53448	2.1209	3.0624	7.03117			
			MILO (Fixed)	2.76	11.25	18.97	35.79	0.150245	0.91737	1.82648	5.4379			
			MILO	4.64	24.39	35.16	55.02	0.19173	0.91737	1.82648	5.4379			
			FULL (skyline for test accuracy)	56.32	56.32	56.32	56.32	17.2387	17.2387	17.2387	17.2387			
			RANDOM (skyline for training time)	2.84	10.52	17.57	35.68	0.150245	0.91737	1.826483	5.437941			
ADAPTIVE-RANDOM (skyline for training time)	0.6067	15.99	33.19	53.3	0.1710	0.91737	1.82648	5.43794						

Table 7: Data Selection Results for CIFAR10, CIFAR100 and TINYIMAGENET datasets

Model Training Standard Deviation Results on Vision Datasets						
Dataset	Model	Budget(%)	Test Accuracy Standard Deviation(for 5 runs)			
			1%	5%	10%	30%
		Selection Strategy				
CIFAR10	ResNet18	FULL (skyline for test accuracy)	0.43	0.43	0.43	0.43
		RANDOM (skyline for training time)	0.187	0.127	0.173	0.154
		ADAPTIVE-RANDOM (skyline for training time)	1.981	0.218	1.87	0.0837
		GLISTER	0.76	1.872	5.8721	0.863
		CRAIGPB	9.31	4.831	4.313	0.2841
		GRADMATCHPB	2.041	1.0841	0.7631	0.0736
		MILO (Fixed)	1.471	4.31	4.12	2.191
		MILO	0.762	1.712	0.0821	0.037
CIFAR10	ResNet101	FULL (skyline for test accuracy)	0.3606	0.3606	0.3606	0.3606
		RANDOM (skyline for training time)	0.141	0.1527	0.1424	0.077
		ADAPTIVE-RANDOM (skyline for training time)	1.295	0.198	1.28	0.063
		GLISTER	0.51	10.27	5.56	0.37
		CRAIGPB	3.804	5.996	2.729	0.2051
		GRADMATCHPB	2.086	0.5374	0.02	0.16
		MILO (Fixed)	3.84	5.64	6.13	1.01
		MILO	2.093	3.691	0.03	0.02
CIFAR100	ResNet18	FULL (skyline for test accuracy)	0.3986	0.3986	0.3986	0.3986
		RANDOM (skyline for training time)	0.2848	0.9871	0.637	0.7168
		ADAPTIVE-RANDOM (skyline for training time)	0.539	0.2546	0.176	0.3915
		GLISTER	0.516	1.32	0.1473	0.08
		CRAIGPB	0.5798	0.8132	0.3323	0.1626
		GRADMATCHPB	0.7637	0.3536	1.039	0.6293
		MILO (Fixed)	0.049	0.56	0.69	0.84
		MILO	0.8211	0.3353	0.1041	0.39
CIFAR100	ResNet101	FULL (skyline for test accuracy)	0.31	0.31	0.31	0.31
		RANDOM (skyline for training time)	0.2716	1.213	1.273	0.891
		ADAPTIVE-RANDOM (skyline for training time)	0.831	0.628	0.583	0.846
		GLISTER	0.631	1.172	0.31	1.23
		CRAIGPB	0.831	1.731	0.347	0.541
		GRADMATCHPB	0.642	0.24	0.53	0.62
		MILO (Fixed)	0.192	0.0931	0.041	0.47
		MILO	1.013	0.764	0.453	0.036
TinyImageNet	ResNet18	FULL (skyline for test accuracy)	0.51	0.51	0.51	0.51
		RANDOM (skyline for training time)	0.53	0.872	0.41	0.73
		ADAPTIVE-RANDOM (skyline for training time)	0.41	0.763	0.31	0.63
		GLISTER	0.125	0.45	0.45	0.17
		CRAIGPB	2.31	0.47	0.51	0.21
		GRADMATCHPB	0.73	0.23	0.46	0.53
		MILO (Fixed)	0.32	0.43	0.24	0.53
		MILO	0.53	0.41	0.32	0.41
TinyImageNet	ResNet101	FULL (skyline for test accuracy)	0.34	0.34	0.34	0.34
		RANDOM (skyline for training time)	0.65	0.43	0.41	0.53
		ADAPTIVE-RANDOM (skyline for training time)	0.64	0.31	0.24	0.41
		GLISTER	0.53	0.741	0.452	0.371
		CRAIGPB	0.872	0.735	0.472	0.531
		GRADMATCHPB	0.764	0.31	0.42	0.53
		MILO (Fixed)	0.736	0.24	0.43	0.45
		MILO	0.41	0.24	0.41	0.431

Table 8: Standard Results for CIFAR10, CIFAR100 and TINYIMAGENET datasets

Model Training Results on Text Datasets										
Dataset	Model	Budget (%)	Top-1 Test accuracy of the Model(%)			Model Training time(in secs)				
			1%	5%	10%	30%	1%	5%	10%	30%
TREC6	LSTM	Selection Strategy FULL (skyline for test accuracy) RANDOM (skyline for training time) ADAPTIVE-RANDOM (skyline for training time)	86.6	86.6	86.6	86.6	101.835	101.835	101.835	101.835
			40.2	62.93	72.27	80.93	1.61	5.83	10.185	31.23
			28.13	61.0	81.53	85.03	1.623	5.82	10.171	31.46
		GLISTER CRAIGPB GRADMATCHPB MILO (Fixed) MILO	24.52	65.45	84.21	86.21	12.621	17.825	19.452	46.742
			25.53	52.87	83.47	85.43	33.83	39.841	43.957	60.742
			23.04	69.93	85.0	87.0	8.621	14.363	18.553	43.848
			34.2	66.07	69.26	81.05	1.614	5.72	10.174	31.22
			46.87	76.13	84.3	87.97	1.613	5.81	10.182	31.21
			89.03	89.03	89.03	89.03	613.553	613.553	613.553	613.553
			50.01	50.01	79.14	84.42	6.789	37.07	63.86	192.587
			49.99	60.04	88.13	88.29	6.673	37.14	63.88	193.632
			50.02	61.25	85.21	86.81	110.242	137.256	166.839	300.512
50.02	66.73	87.54	87.7	118.553	137.256	166.839	295.567			
50.02	58.99	84.66	85.75	99.116	137.256	166.839	347.057			
50.03	66.54	81.3	85.06	6.791	37.06	63.86	192.59			
50.02	69.15	88.45	88.56	6.81	37.1	63.89	192.57			
Rotten Tomatoes	LSTM	Selection Strategy FULL (skyline for test accuracy) RANDOM (skyline for training time) ADAPTIVE-RANDOM (skyline for training time)	79.54	79.54	79.54	79.54	177.656	177.656	177.656	177.656
			52.43	67.39	69.08	73.82	2.305	9.274	18.159	56.883
			49.91	68.44	78.22	79.47	1.8730	9.258	18.163	56.914
		GLISTER CRAIGPB GRADMATCHPB MILO (Fixed) MILO	50.01	50.54	65.43	78.13	10.23	14.23	26.24	110.31
			50.04	50.81	62.45	77.21	12.84	16.94	29.31	124.21
			49.99	50.0	63.24	78.08	9.641	13.184	25.623	102.789
			50.7	67.13	72.43	74.38	1.87	9.28	18.2	56.90
			50.93	73.76	78.31	79.52	1.89	9.74	18.34	56.781
			93.27	93.27	93.27	93.27	5695.329	5695.329	5695.329	5695.329
			51.25	228.316	601.866	1672.21	87.362	89.58	90.33	91.91
			51.25	228.316	601.866	1672.21	89.813	92.18	92.41	92.93
			86.25	91.21	92.01	92.43	721.43	789.21	898.31	1802.74
86.31	90.46	91.85	91.99	868.42	925.32	981.321	1831.31			
86.54	90.42	91.99	91.83	682.987	758.215	892.21	1792.43			
86.15	89.27	90.87	91.458	51.25	228.316	601.866	1672.21			
90.76	92.06	92.6	93.144	51.25	228.316	601.866	1672.21			

Table 9: Model Training Results for TREC6, IMDB and Rotten Tomatoes datasets

Test Accuracy Standard Deviation on Text Datasets							
Dataset	Model	Budget(%)	Selection Strategy	Standard deviation of the Model(for 5 runs)			
				1%	5%	10%	30%
TREC6	LSTM	FULL (skyline for test accuracy)	FULL (skyline for test accuracy)	0.77	0.77	0.77	0.77
			RANDOM (skyline for training time)	3.41	1.23	0.57	1.34
			ADAPTIVE-RANDOM (skyline for training time)	3.2	0.43	1.31	0.43
		GLISTER	GLISTER	2.45	0.74	0.31	0.54
			CRAIGPB	0.791	0.462	1.821	0.861
			GRADMATCHPB	1.7265	0.8762	0.472	0.876
			MILO (Fixed)	0.352	0.62	0.454	0.726
			MILO	0.25	0.36	0.21	0.31
IMDB	LSTM	FULL (skyline for test accuracy)	FULL (skyline for test accuracy)	0.3	0.3	0.3	0.3
			RANDOM (skyline for training time)	0.21	0.31	0.41	1.2
			ADAPTIVE-RANDOM (skyline for training time)	1.241	0.21	0.41	0.21
		GLISTER	GLISTER	0.862	0.21	0.21	0.1
			CRAIGPB	0.731	1.21	0.451	0.41
			GRADMATCHPB	0.817	0.441	0.41	1.22
			MILO (Fixed)	1.51	0.42	0.34	0.51
			MILO	0.45	0.21	0.104	0.05
Rotten Tomatoes	LSTM	FULL (skyline for test accuracy)	FULL (skyline for test accuracy)	0.34	0.34	0.34	0.34
			RANDOM (skyline for training time)	1.21	1.41	1.97	0.31
			ADAPTIVE-RANDOM (skyline for training time)	0.0871	0.16	0.31	0.21
		GLISTER	GLISTER	0.761	0.43	0.34	0.31
			CRAIGPB	0.826	0.12	0.43	0.41
			GRADMATCHPB	0.52	0.2	0.21	0.12
			MILO (Fixed)	0.7761	0.31	0.1	0.31
			MILO	0.71	0.41	0.1	0.21
IMDB	BERT+MLP	FULL (skyline for test accuracy)	FULL (skyline for test accuracy)	0.14	0.14	0.14	0.14
			RANDOM (skyline for training time)	0.38	0.981	1.31	0.21
			ADAPTIVE-RANDOM (skyline for training time)	0.21	0.24	0.31	0.51
		GLISTER	GLISTER	0.871	0.31	0.53	0.72
			CRAIGPB	0.87	0.66	0.2	0.731
			GRADMATCHPB	0.54	0.53	0.23	0.61
			MILO (Fixed)	0.21	0.21	0.12	0.3
			MILO	0.43	0.12	0.3	0.12

Table 10: Standard Deviation Results for TREC6, IMDB and Rotten Tomatoes datasets

Hyper-parameter Ordering Retention Capabilit				
Dataset	Model	Budget	Strategy	Kendall Tau Values
TREC6	LSTM	1%	MILO	<b>0.4321</b>
			RANDOM	0.0679
			ADAPTIVE-RANDOM	0.313
			AUTOMATA	0.3484
			CRAIGPB	0.325
		5%	MILO	<b>0.521</b>
			RANDOM	0.199
			ADAPTIVE-RANDOM	0.440
			AUTOMATA	0.4764
			CRAIGPB	0.4521
		10%	MILO	<b>0.6342</b>
			RANDOM	0.2605
			ADAPTIVE-RANDOM	0.5313
			AUTOMATA	0.4742
			CRAIGPB	0.4531

Table 11: Mean test set accuracy of ResNet18 trained on CIFAR100 dataset for subset sizes of 10%, and 30% selected using MILO for 200 epochs for different values of  $R$ .

		Hyper-parameter Tuning Results										
Dataset	Model	Search+Schedular	Budget(%)	Top-1 Test accuracy of the Model(%)			Tuning time(in hrs)					
				1%	5%	10%	30%	1%	5%	10%	30%	
TREC6	LSTM	Search+Scheduler Random+HB	Selection Strategy FULL (skyline for test accuracy) RANDOM (skyline for training time) ADAPTIVE-RANDOM (skyline for training time) 45.76	86.8	86.8	86.8	86.8	0.64	0.64	0.64	0.64	0.64
				40.8	60.2	78.0	85.5	0.01	0.03	0.07	0.18	
				49.43	74.32	86.6	0.01	0.03	0.06	0.18		
TREC6	LSTM	TPE+HB	FULL (skyline for test accuracy) RANDOM (skyline for training time) ADAPTIVE-RANDOM (skyline for training time)	41.33	64.33	77.0	82.0	0.02	0.07	0.08	0.19	
				47.3	66.2	82.0	86.6	0.01	0.06	0.09	0.21	
				54.32	79.83	85.51	86.43	0.01	0.04	0.06	0.18	
TREC6	LSTM	MILo (Fixed)	MILo	76.2	86.6	86.54	86.6	0.01	0.03	0.06	0.18	
				84.4	84.4	84.4	84.4	0.64	0.64	0.64	0.64	
				40.8	60.2	78	85.5	0.01	0.03	0.06	0.18	
TREC6	LSTM	MILo (Fixed)	MILo	52.32	64.32	79.2	83.42	0.01	0.04	0.06	0.18	
				41.33	64.33	77	82	0.02	0.07	0.08	0.19	
				47.2	66.2	82	86.6	0.01	0.06	0.09	0.21	
CIFAR10	ResNet18	Random+HB	FULL (skyline for test accuracy) RANDOM (skyline for training time) ADAPTIVE-RANDOM (skyline for training time)	68.2	84.26	84.34	86.46	0.01	0.03	0.06	0.18	
				95.35	95.35	95.35	95.35	36.11	36.11	36.11	36.11	
				87.21	88.95	90.21	94.21	0.4779	1.8681	3.7917	10.900	
CIFAR10	ResNet18	TPE+HB	FULL (skyline for test accuracy) RANDOM (skyline for training time) ADAPTIVE-RANDOM (skyline for training time)	93.1	94.32	94.78	95.21	0.47790	1.86814	3.79172	10.9002	
				92.43	93.5	94.2	94.3	0.5434	1.92925	3.83061	11.06829	
				93.7	93.8	94.21	95.31	0.67548	1.91481	3.81394	11.0127	
CIFAR10	ResNet18	MILo (Fixed)	MILo	86.21	88.95	94.21	95.21	0.47790	1.868144	3.791	10.909	
				94.34	95.34	95.21	95.34	0.4778	1.8644	3.796	10.9889	
				95.24	95.24	95.24	95.24	36.12	36.12	36.12	36.12	
CIFAR10	ResNet18	MILo (Fixed)	MILo	86.38	89.32	92.21	94.21	0.48	1.87	3.79	10.9	
				93.12	93.72	94.78	95.21	0.49	1.89	3.78	11.1	
				92.23	93.5	94.2	94.3	0.54	1.93	3.83	11.07	
CIFAR10	ResNet18	TPE+HB	FULL (skyline for test accuracy) RANDOM (skyline for training time) ADAPTIVE-RANDOM (skyline for training time)	93.7	93.98	94.21	95.31	0.68	1.91	3.81	11.01	
				87.11	90.21	94.21	95.21	0.48	1.87	3.79	10.9	
				93.24	94.28	95.1	95.21	0.52	1.89	3.77	10.89	

Table 12: Hyper-parameter Tuning Results